Analytical and numerical adjoint solutions for cumulative streamflow depletion

Chris Turnadge[1,2,3*], Roseanna M. Neupauer[4], Okke Batelaan[1,2], Russell S. Crosbie[3], Craig T. Simmons[2,5]

[1] College of Science and Engineering, Flinders University, Bedford Park, SA 5042, Australia.

[2] National Centre for Groundwater Research and Training, Flinders University, GPO Box 2100, Adelaide, SA 5001, Australia.

[3] CSIRO Environment, Locked Bag No. 2, Glen Osmond, SA 5064, Australia.

[4] Department of Civil, Environmental and Architectural Engineering, University of Colorado, Boulder, CO 80309, U.S.A.

[5] College of Engineering, Science and Environment, University of Newcastle, University Drive, Callaghan, NSW 2308, Australia.

* Corresponding author: Chris Turnadge (Chris.Turnadge@csiro.au)

Key Points:

- New analytical solutions for cumulative streamflow depletion were derived
- A new numerical adjoint solution for cumulative streamflow depletion was derived
- The derived adjoint solution can be orders of magnitude more efficient than traditional perturbation-based approaches to estimating cumulative streamflow depletion

Abstract

Streamflow depletion is traditionally defined as the instantaneous change in the volumetric rate of aquifer–stream exchange after a finite period of continuous groundwater extraction. In the present study an alternative metric of streamflow depletion was considered: cumulative stream depletion (CSD), which described the total volumetric reduction in flow from an aquifer to a stream resulting from continuous groundwater extraction over a finite period. A novel analytical solution for the prediction of CSD was derived, based upon an existing solution that accounted for streambed conductance and partial stream penetration. Separately, a novel numerical solution for the prediction of CSD was derived, based on the derivation of an adjoint state solution. The accuracy of the two new solutions was demonstrated through benchmarking against existing analytical solutions and perturbation-based results, respectively. The derivation of the loading term used in the adjoint state solution identified three parameters of relevance to CSD prediction. First is streambed hydraulic conductivity and thickness, both of which contribute to a lumped parameterization of streambed conductance. Second is aquifer specific yield, which controls the rate at which hydraulic perturbations propagate through an aquifer. The computational advantage of the adjoint state approach was highlighted, in which a single numerical model run can be used to predict CSD resulting from any potential groundwater extraction location. The reduction in computation time achieved was proportional to the number

of potential extraction well locations. Where the number of locations is large, reductions in computation times of nearly 100 % can be achieved.

1. Introduction

Streamflow depletion traditionally describes a reduction in flow between an aquifer and a connected, gaining stream resulting from groundwater extraction (Barlow and Leake, 2012). This concept can be generalised to losing streams, where increases in stream discharge may occur, as well as to other surface water features such as rivers and lakes. Streamflow depletion can result in the reduction or cessation of aquifer–stream exchange fluxes. Where streams provide potable water supplies for municipal, domestic, or agricultural uses, reductions in baseflow can put the security of such supplies at risk. Reductions to in-stream flow regimes and the resulting changes to water chemistry can also cause considerable negative ecological impacts.

1.1. Instantaneous streamflow depletion

Traditionally, streamflow depletion was conceptualized as the reduction in groundwater discharge to a stream (Q_S) resulting from continuous groundwater extraction at a rate (Q_B) over a finite period (e.g., from t_0 to t_f), at the end of the extraction period (t_f); i.e.:

$$Q_{ISD}(t_f) = \Delta Q_S = \frac{dQ_S(t_f)}{dQ_B} Q_B \tag{1}$$

where $Q_{ISD}(t_f)$ is instantaneous streamflow depletion (ISD, $L^3.T^{-1}$) and Q_S is the exchange flow across the streambed sediment ($L^3.T^{-1}$), given by:

$$\begin{aligned} Q_S(t) &= \int_S C_S(\mathbf{x}) \left[h(\mathbf{x},t) - h_S(\mathbf{x},t)\right] \, ds \\ &= \int_\Omega \frac{K_S(\mathbf{x})}{b_S(\mathbf{x})} \left[h(\mathbf{x},t) - h_S(\mathbf{x},t)\right] A_S(\mathbf{x}) \, d\mathbf{x} \end{aligned} \tag{2}$$

where h is aquifer hydraulic head, h_S is stream stage, s represents the centreline of the stream, Ω represents the spatial domain, A_S is a dimensionless indicator function that has a value of unity along streams and zero elsewhere. C_S is a lumped parameter known as streambed conductance ($L.T^{-1}$), defined as:

$$C_S(\mathbf{x}) = \frac{K_S(\mathbf{x})\, W_S(\mathbf{x})}{b_S(\mathbf{x})} \tag{3}$$

where K_S is streambed hydraulic conductivity ($L.T^{-1}$), W_S is streambed wetted perimeter (L), and b_S is streambed thickness (L). Following this definition, streambed conductance features units of ($L.T^{-1}$) (e.g. Neupauer et al., 2021), rather than ($L^2.T^{-1}$) (e.g. Brunner et al., 2010). The inclusion of the function A_s in equation (2) ensures that, while integration is performed over the entire model domain (i.e., Ω), stream–aquifer exchange occurs only at stream locations. When numerical solution methods are used, appropriate specification of the terms W_S and b_S is necessary to ensure accurate prediction of streamflow depletion (Mehl and Hill, 2010). Streambed conductance values can be estimated through inversion of simultaneous observations of stream flow, stream stage, and aquifer hydraulic head. Alternatively, the component parameters of the streambed conductance term can be estimated independently using laboratory testing methods, such as streambed sediment particle size distribution analyses (Fox et al., 2011), or from field observations, such as falling head permeameter testing (Landon et al., 2001; Fox, 2004). Existing analytical and numerical methods of estimating ISD are summarized as follows.

1.2. Analytical solutions for instantaneous streamflow depletion

A vast number of analytical and semi-analytical solutions for the first-order prediction of ISD have been developed since the 1940s (Hunt, 2014; Huang et al., 2018), of which a handful have been widely implemented. The seminal ISD solution was derived by Theis (1941), the

calculation of which was subsequently simplified by Glover and Balmer (1954). This solution featured a relatively large number of assumptions, including: the absence of a streambed conductance layer; that the stream and well both fully penetrate the aquifer; that hydraulic properties are homogeneous; and that extraction is continuous. Theis (1941) and Glover and Balmer (1954) presented a closed-form analytical solution for the estimation of depletion of unconfined groundwater flow to a fully connected, fully penetrating stream featuring no resistance to flow (i.e., zero streambed thickness). Theis (1941) and Glover and Balmer (1954) extended the Theis (1935) drawdown solution via the inclusion of an infinitely long Dirichlet boundary condition of infinitesimal width to represent a stream boundary. This conceptualization of ISD and its corresponding solution will hereafter be referred to as the "TGB solution". The TGB solution describes instantaneous streamflow depletion (Q_{ISD}) at time t_f resulting from continuous groundwater extraction from t_0 to t_f as:

$$Q_{ISD}(t_f) = Q_B \operatorname{erfc}\left[\sqrt{\frac{(\Delta x)^2 S_y}{4 T t_f}}\right] \quad (4)$$

where Δx is well-stream separation distance (L), t_f is the time since the onset of extraction at which ISD is calculated (which is equal to the duration of time elapsed) (T), T is aquifer transmissivity ($L^2.T^{-1}$), S_y is aquifer specific yield (unitless) and erfc is the complementary error function. In practice, a constant aquifer thickness is used to calculate a representative T value. Importantly, this requires the assumption that the reduction in aquifer saturated thickness due to extraction (i.e., drawdown) is negligible with respect to total aquifer thickness.

Hantush (1965) extended the TGB solution to include the presence of a relatively lower hydraulic conductivity conductance layer between the pumped aquifer and the stream (i.e., non-

zero streambed thickness). The remainder of the assumptions of the TGB solution were retained, including full aquifer penetration of both the production well and stream. This conceptualization will hereafter be referred to as the "Hantush solution". The Hantush solution described instantaneous streamflow depletion at time t_f resulting from continuous groundwater extraction as:

$$Q_{ISD}(t_f) = Q_B \left\{ \operatorname{erfc}\left[\sqrt{\frac{(\Delta x)^2\, S_y}{4\, T\, t_f}}\right] - \exp\left[\frac{T\, t_f}{S_y\, R^2} + \frac{\Delta x}{R}\right] \operatorname{erfc}\left[\sqrt{\frac{T\, t_f}{S_y\, R^2}} + \sqrt{\frac{(\Delta x)^2\, S_y}{4\, T\, t_f}}\right] \right\} \quad (5)$$

where exp is the exponential function and $R = K\, b_S \,/\, K_S$, where K is aquifer hydraulic conductivity ($L.T^{-1}$).

Hunt (1999) derived a solution that accounted for the effects of a streambed conductance layer, a partially penetrating stream, and a partially penetrating well. This conceptualization will hereafter be referred to as the "Hunt solution". The Hunt solution described instantaneous streamflow depletion at time t_f resulting from continuous groundwater extraction as:

$$\begin{aligned} Q_{ISD}(t_f) = Q_B \Bigg\{ & \operatorname{erfc}\left[\sqrt{\frac{(\Delta x)^2\, S_y}{4\, T\, t_f}}\right] \\ & - \exp\left[\frac{\lambda^2\, t_f}{4\, S_y\, T} + \frac{\lambda\, \Delta x}{2\, T}\right] \operatorname{erfc}\left[\sqrt{\frac{\lambda^2\, t}{4\, S_y\, T}} + \sqrt{\frac{(\Delta x)^2\, S_y}{4\, T\, t}}\right] \Bigg\} \end{aligned} \quad (6)$$

where λ is related to streambed conductance. For example, when defined as $\lambda = C_S(\mathbf{x}) = K_S(\mathbf{x})\, W_S(\mathbf{x}) \,/ b_S(\mathbf{x})$ (per equation 3), the Hunt solution is equivalent to the Hantush solution. It is assumed that the stream is fully hydraulically connected to the watertable aquifer at all times (Brunner et al., 2011).

Other ISD solutions addressed a range of unique hydrogeological conceptualisations. Unconfined conditions were most commonly simulated, although confined conditions were often assumed in order to simplify (i.e., linearize) governing equations. Solutions for leaky aquifers (Hunt, 2003; Butler et al., 2007; Zlotnik and Tartakovsky, 2008; Zlotnik, 2004) and multi-layer flow systems (Hunt, 2009; Ward and Lough, 2011; Ward and Falle, 2012) were also derived. Aquifer geometries considered included infinite (Fox et al., 2002) or semi-infinite (Hunt, 2003) domains, as well as rectangular (Chan, 1976; Huang et al., 2014, 2015), wedge-shaped (Chan et al., 1978; Yeh and Chang, 2006; Sedghi et al., 2009) or strip aquifers (Jenkins, 1968; Butler et al., 2001; Miller et al., 2007; Sun and Zhan, 2007; Zlotnik, 2014). In addition to fully penetrating vertical wells, ISD solutions for other well construction geometries included partially penetrating vertical wells (Hunt, 1999) and non-vertical wells (Tsou et al., 2010). Constant extraction rates were typically assumed, although transient extraction was also considered, including cyclic extraction schemes (Wallace et al., 1990; Darama, 2001; Neupauer et al., 2023a). Streams were typically simulated as featuring a single linear geometry, but also included multiple parallel streams (Sun and Zhan, 2007), as well as curvilinear streams (Huang and Yeh, 2015) or right-angled streams (Hantush, 1967). Partial aquifer penetration of streams was addressed by Butler et al., (2001) and Chen and Yin (2004).

While many solutions assumed constant stream stage values, spatio-temporal variations in stream stage (Intaraprasong and Zhan, 2009) and streambed conductance (Neupauer et al., 2021) have also been considered. Solutions that considered streams featuring finite widths were derived by Butler et al. (2001) and Hunt (2008). In addition to their use as forward models for the prediction of instantaneous streamflow depletion, analytical ISD solutions have also been used to inversely estimate hydrogeological and streambed parameters. For example, Christensen

(2000) and Lough and Hunt (2006) used the Hunt (1999) and Hunt (2003) ISD solutions, respectively, to inversely estimate aquifer transmissivity and specific yield values, as well as streambed conductance values. Analytical ISD solutions were implemented in software such as STRMDEPL08 (Reeves, 2008) and the streamDepletr package for R (Zipper et al., 2019).

1.3. Numerical solutions for instantaneous streamflow depletion

Numerical groundwater flow solutions are commonly used to assess ISD in contexts where sufficient data and/or subsurface complexity warrant the development of a numerical forward model. Numerical solutions feature far fewer assumptions than their analytical counterparts. For this reason, numerical solutions can be used to represent more complex conceptualisations and parameterizations, including irregular geometry and heterogeneous parameters that vary in space and/or time.

1.3.1. Perturbation solutions

Paired numerical forward models can be used to calculate ISD as the difference between aquifer–stream exchange fluxes using a perturbation approach. The perturbation approach involves solving an appropriate form of the groundwater flow equation using a defined set of parameter values; e.g., from the minimization of discrepancies between modelled and measured flow system states. Additional solutions are then obtained for each perturbation of interest. For the specific case of streamflow depletion, additional solutions are obtained for each potential extraction well location. Instantaneous streamflow depletion is then calculated as the difference in aquifer–stream exchange flux between (1) the original model and (2) each perturbed model. When using the perturbation approach to assess ISD, the number of additional model runs required is equal to the number of potential extraction locations.

1.3.2. Adjoint solutions

The development of the adjoint state approach across various scientific and engineering disciplines is first briefly summarized as follows. Use of the adjoint state approach to calculate model sensitivities equations was first formalized for application to both linear and nonlinear systems by Cacuci (1981a, 1981b). This followed a number of diverse implementations in fields such as nuclear engineering (Wigner, 1945; Weinberg and Wigner, 1958; Gandini, 1967), reservoir engineering (Jacquard and Jain, 1965; Carter et al., 1974; Chavent et al., 1975) and meteorology (Marchuk, 1975). The adjoint state approach to sensitivity analysis and optimal control has been described in monographs such as Marchuk (1994), Cacuci (2003), and Cacuci et al. (2005). Adjoint state approaches were first applied to problems in groundwater hydrology by Vemuri and Karplus (1969), Neuman and Yakowitz (1979) and Neuman et al. (1980). The framework for the application of adjoint solutions to saturated groundwater flow problems was later derived for steady (Sykes et al. 1985) and for transient (Wilson and Metcalfe, 1985) flow conditions. The method was used to calculate the sensitivities of saturated (Townley and Wilson, 1985; Wilson and Metcalfe, 1985) and unsaturated (Kabala and Milly, 1990; Lehmann and Ackerer, 1997) groundwater flow solutions, and of solute transport solutions (Ahlfeld et al., 1988a, 1988b; Neupauer and Wilson 1999, 2001).

Adjoint state methods of calculating model sensitivities are often more efficient than their perturbation-based counterparts. In many cases, the output of a single, additional adjoint model run can be combined with existing forward model outputs to calculate the sensitivity of a given model output to a range of parameters. For the specific case of instantaneous streamflow depletion, the adjoint approach allows estimates to be calculated at all potential groundwater extraction locations using only a single adjoint state model run. Adjoint state methods were first

used to calculate instantaneous streamflow depletion solutions by Neupauer and Griebling (2012) and Griebling and Neupauer (2013). These studies featured relatively complex, multi-layered hydrogeological flow systems featuring irregular geometries and nonlinear groundwater-surface water exchange mechanisms, as well as the evapotranspiration of shallow groundwater. The efficiency of the adjoint approach was shown in these studies to exceed that of the perturbation method by a factor of 250; i.e., by more than two orders of magnitude.

1.4. Cumulative streamflow depletion

The metric of instantaneous streamflow depletion represents the change in the volumetric rate of aquifer–stream exchange and therefore has units of $L^3.T^{-1}$. At a local scale this metric is appropriate, since it can be related to measurable rates of volumetric flow for processes located within both the stream and aquifer domains at a particular study location. However, conjunctive management of surface and groundwater resources at regional scales typically involves estimation of volumetric water balances, which are often averaged over finite (e.g., annual) time periods. This requires the integration of ISD through time, in order to estimate a total net annual volume that can be related to other water balance components. For this reason, an alternative metric of streamflow depletion was considered in the present study: cumulative stream depletion (CSD). This refers to the total volumetric reduction in flow from an aquifer to a stream (V_{CSD}) resulting from continuous groundwater extraction over a finite period (i.e., from t_0 to t_f), at the end of the extraction period (t_f); i.e.:

$$V_{CSD}(t_f;\mathbf{x}_B) = \int_{t_0}^{t_f} Q_{ISD}(t;\mathbf{x}_B)\,dt = Q_B \int_{t_0}^{t_f} \frac{dQ_S(t;\mathbf{x}_B)}{dQ_B(t;\mathbf{x}_B)}\,dt \tag{7}$$

Cumulative stream depletion represents the cumulative volume of water that would otherwise have discharged to a stream in the absence of groundwater extraction. In comparison to the vast

number of existing ISD solutions, closed-form analytical solutions for the estimation of CSD do not currently exist. Instead, CSD is typically estimated through either: (1) the temporal integration of analytical ISD solutions using numerical methods, which can be cumbersome and potentially subject to discretization errors; or (2) numerical solutions of the groundwater flow equation. In the present study, two new cumulative streamflow depletion solutions were derived: one closed-form analytical solution and one numerical adjoint solution. The analytical solution is suited to assessments of CSD in data poor areas or is suitable for didactic purposes. As a numerical solution, the adjoint solution features relatively fewer assumptions and is therefore suitable for assessments of CSD in data rich and/or hydrogeologically complex contexts. An additional key benefit of the adjoint solution is the ability to use a single numerical model run to assess CSD resulting from any potential extraction location.

2. Methods

The numerical integration of analytical ISD solutions was used to provide benchmarks against which new analytical and numerical adjoint solutions were compared for three flow system conceptualizations. The Hunt (1999) analytical solution for ISD was used as the basis for derivation of a new closed-form analytical solution for CSD, which is appropriate for use in data poor investigations. A new numerical adjoint solution was also derived for the calculation of CSD, which is appropriate for use in data rich investigations. This was compared to both numerically integrated ISD solutions and the analytical CSD solution in a relatively simple application. The numerical adjoint CSD solution was also compared to perturbation-based numerical solutions in a relatively complex application.

2.1. Forward model

The governing equation for two-dimensional groundwater flow in a heterogeneous, anisotropic unconfined aquifer featuring stream–aquifer exchange and non-head-dependent source/sink terms is an extended version of the Boussinesq equation (Bear, 1979):

$$-S_y(\mathbf{x},t)\,\frac{\partial h(\mathbf{x},t)}{\partial t} + \nabla\cdot[\mathbf{K}(\mathbf{x},t)\,h(\mathbf{x},t)\,\nabla h(\mathbf{x},t)] - \frac{K_s}{b_s}[h(\mathbf{x},t) - h_s(\mathbf{x},t)]\,A_S(\mathbf{x}) - Q_B(\mathbf{x},t)\,\delta(\mathbf{x}-\mathbf{x}_B) + N(\mathbf{x},t) = 0 \quad (8)$$

where $\mathbf{x}=[x,y]$, S_y is aquifer specific yield (unitless), h is aquifer hydraulic head (L), the ∇ operator represents divergence in x and y dimensions, $\mathbf{K}$ is a 2-D tensor of aquifer hydraulic conductivity values ($L.T^{-1}$), A_S is a dimensionless indicator function with a value of unity along the stream network and a value of zero elsewhere, Q_B represents groundwater extractions ($L^3.T^{-1}$) at locations $\mathbf{x}_B$, and N represents spatially distributed non-head-dependent source terms ($L.T^{-1}$), including recharge. A key assumption of the Boussinesq equation is that vertical flow velocities are small in comparison to their horizontal counterparts; i.e., Dupuit-Forchheimer conditions. To increase the tractability of solving this governing equation, it can be further simplified by assuming that drawdown resulting from extraction is small in comparison to the saturated thickness of the unconfined aquifer. The resulting linearized two-dimensional governing equation is therefore (Hunt, 1999):

$$-S_y\frac{\partial h(\mathbf{x},t)}{\partial t} + \nabla\cdot[\mathbf{T}\,\nabla h(\mathbf{x},t)] - \frac{K_S}{b_S}[h(\mathbf{x},t) - h_S(\mathbf{x},t)]\,A_S(\mathbf{x}) - Q_B\,\delta(\mathbf{x}-\mathbf{x}_B) + N(\mathbf{x},t) = 0 \quad (9)$$

where $\mathbf{T}$ is a 2-D tensor of aquifer transmissivity values [$L^2.T^{-1}$], in which elements are defined as $T_{ij} = K_{ij}(h - z_{bot})$, where z_{bot} is the elevation of the base of the aquifer. Again, each term contained in this governing equation has units of $L.T^{-1}$. This simplified formulation also enabled

comparisons of the new analytical and numerical adjoint solutions derived in the present study to previously published analytical streamflow depletion solutions, which were based on the same simplifying assumptions. This simplified governing equation can be solved using one more of the following boundary conditions:

$$h(\mathbf{x},t) = g_1(\mathbf{x},t) \text{ where } \mathbf{x} \in \Gamma_1 \quad (10)$$

$$\nabla h(\mathbf{x},t) \cdot \mathbf{n} = g_2(\mathbf{x},t) \text{ where } \mathbf{x} \in \Gamma_2 \quad (11)$$

$$[\alpha\, h\,(\mathbf{x},t) - \mathbf{T}\,\nabla h(\mathbf{x},t)] \cdot \mathbf{n} = g_3(\mathbf{x},t) \text{ where } \mathbf{x} \in \Gamma_3 \quad (12)$$

and the initial condition:

$$h(\mathbf{x},t) = h_0(\mathbf{x}) \text{ where } t = t_0 \quad (13)$$

where g_1, g_2, g_3 are known functions of $\mathbf{x}$ and t, α ($\mathrm{L.T^{-1}}$) is a flow conductance parameter, and $h_0(\mathbf{x})$ is the initial condition specified at $\mathbf{x}$. Specifically, first-type (Dirichlet) conditions represent boundaries (Γ_1) along which hydraulic head values remain constant in time. Second-type (Neumann) conditions represent boundaries (Γ_2) along which an inward or outward flux remains constant in time. Third-type (Cauchy) conditions represent boundaries (Γ_3) along which an inward or outward flux is dependent upon the gradient between aquifer hydraulic head on the boundary and an external hydraulic head value and mediated by a flow conductance parameter.

2.2. Numerical integration of existing ISD solutions

The numerical integration of analytical ISD solutions provided a benchmark against which other solutions were compared. The Theis, Hantush, and Hunt ISD solutions were numerically integrated using Clenshaw–Curtis quadrature, which was implemented using the SciPy library for Python (Virtanen et al., 2020). Absolute discrepancies were calculated as the arithmetic difference between the results of alternative methods and those of numerical

integration. Percent difference discrepancies were expressed as a proportion of absolute discrepancies calculated by numerical integration.

2.3. Derivation of a new analytical CSD solution

A closed-form solution for the total volume of cumulative streamflow depletion (V_{CSD}) resulting from continuous groundwater extraction over a finite period (i.e., from t_0 to t_f), at the end of the extraction period (t_f), was derived through temporal integration of equation (6):

$$\begin{aligned} V_{CSD}(t_f;\Delta x) = \; Q_B \Bigg\{ & \left(2\,G^2 + t_f + \frac{1}{H^2} + \frac{2\,G}{H}\right) \operatorname{erfc}\left(\frac{G}{\sqrt{t_f}}\right) \\ & - \frac{e^{2\,G\,H + H^2 t_f}}{H^2} \operatorname{erfc}\left(\frac{G}{\sqrt{t_f}} + H\sqrt{t_f}\right) - \frac{2\,(G\,H+1)}{H\,\sqrt{\pi}} \sqrt{t_f}\, e^{-G^2/\,t_f} \\ & - \left(2\,G^2 + t_0 + \frac{1}{H^2} + \frac{2\,G}{H}\right) \operatorname{erfc}\left(\frac{G}{\sqrt{t_0}}\right) \\ & + \frac{e^{2\,G\,H + H^2 t_0}}{H^2} \operatorname{erfc}\left(\frac{G}{\sqrt{t_0}} + H\sqrt{t_0}\right) + \frac{2\,(G\,H+1)}{H\,\sqrt{\pi}} \sqrt{t_0}\, e^{-G^2/\,t_0} \Bigg\} \end{aligned} \tag{14}$$

where the coefficient G, which has units of $\sqrt{\mathrm{T}}$, is defined as:

$$G = \sqrt{\frac{(\Delta x)^2\, S_y}{4\,K\,b}} \tag{15}$$

A comprehensive description of the derivation is provided in Electronic Supplementary Material S1. For the TGB case, the value of the H coefficient, which has units of $\sqrt{\mathrm{T}^{-1}}$, is equal to infinity. In practical terms, this means that all terms in equation (14) that are a function of H become zero-valued and can be omitted. For the Hunt case, the H coefficient is defined as:

$$H = \sqrt{\frac{\lambda^2}{4\,S_y\,K\,b}} \tag{16}$$

For the Hantush case, the parameter λ, which has units of L.T^{-1}, is defined specifically as $\lambda = 2\ K_S\ b\ /b_S$; therefore, the H coefficient is defined as:

$$H = \sqrt{\frac{4\ {K_S}^2\ b^2}{b_S^2}\left(\frac{1}{4\ S_y\ K\ b}\right)} = \frac{K_S}{b_S}\sqrt{\frac{b}{S_y\ K}} \tag{17}$$

For the special case where t_0=0, equation (14) can instead be applied as a function of time elapsed since the onset of extraction and all terms dependent on t_0 become zero-valued. Under these conditions, equation (14) simplifies to:

$$V_{CSD}(t_f;\Delta x) = Q_B\left[\left(2\ G^2 + t_f + \frac{1}{H^2} + \frac{2\ G}{H}\right)\ \text{erfc}\left(\frac{G}{\sqrt{t_f}}\right) - \frac{e^{2\ G\ H + H^2 t_f}}{H^2}\ \text{erfc}\left(\frac{G}{\sqrt{t_f}} + H\ \sqrt{t_f}\right) - \frac{2\ (G\ H + 1)}{H\ \sqrt{\pi}}\ \sqrt{t_f}\ e^{-G^2/\ t_f}\right] \tag{18}$$

For a simplified conceptualization featuring a fully penetrating stream and well in the absence of a streambed conductance layer (i.e., which is consistent with the Theis-Glover-Balmer solution for ISD), equation (14) is independent of H and therefore simplifies further to:

$$V_{CSD}(t_f;\Delta x) = Q_B\ \left[\left(2\ G^2 + t_f\right)\ \text{erfc}\left(\frac{G}{\sqrt{t_f}}\right) - \frac{2\ G\sqrt{t_f}\ e^{-G^2/t_f}}{\sqrt{\pi}}\right] \tag{19}$$

The expressions presented in equations (14), (18), and (19) feature two dependent variables (i.e. Δx, t_f) and five parameters (K, S_y, b, K_s, Q_B), each of which are physically-based and are therefore measurable, or able to be estimated or constrained. This parameter space can be reduced by use of dimensionless analysis. Dimensionless CSD (V_{CSD}^*) can be defined by normalizing the total volume of stream-aquifer exchange (V_S) by the total volume of groundwater extracted (V_B) over a given duration of extraction (i.e. $V_{CSD}^* = V_S/V_B$). Dimensionless CSD values can be expressed as a function of dimensionless distance (defined as $(\Delta x)^* = \lambda \Delta x/T$) and dimensionless time (defined as $t^* = 4Tt_f/\left[S_y(\Delta x)^2\right]$). Dimensionless CSD values were

calculated using equation (18) for $\Delta x_D \in (10^{-2}, \infty)$ and $t_D \in (10^{-1}, 10^4)$ (Figure 1). A similar dimensionless analysis for ISD was presented by Hunt (1999, Figure 4). Dimensionless CSD increases sigmoidally as a function of dimensionless time. The rate of increase in V^*_{CSD} over dimensionless time increases as a function of dimensionless distance; therefore, CSD is positively correlated with K_r and Δx, and is negatively correlated with b_r and T. Sigmoidal increases in V^*_{CSD} values over dimensionless time rapidly approach an asymptotic upper limit (at $\Delta x^* = \infty$) for Δx^* values > 0.1. Therefore, CSD estimates are relatively less sensitive to variations in large streambed conductance values, large stream–bore separation distances, and small aquifer transmissivity values.

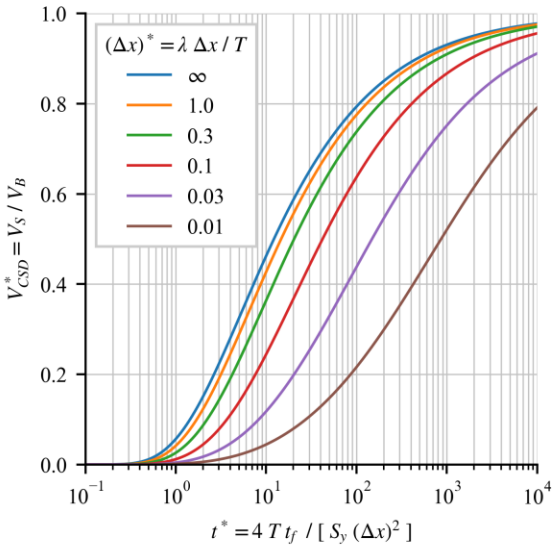

Figure 1. Dimensionless cumulative streamflow depletion (V^*_{CSD}, defined as $V^*_{CSD} = V_S/V_B$) versus dimensionless time (t^*, defined as $t^* = 4\ T\ t_f\ /\ [S_y(\Delta x)^2]$) for selected values of dimensionless distance [$(\Delta x)^*$, defined as $(\Delta x)^* = \lambda\ \Delta x\ /\ T$].

To the authors' knowledge, the solutions presented in equations (14), (18), and (19) have not been derived previously. These equations can be implemented using scripted languages or spreadsheet software and avoid the need for cumbersome numerical integration of existing ISD

299 solutions. These analytical CSD solutions will typically provide conservative predictions of
300 maximum cumulative streamflow depletion, due to assumptions of full stream penetration extent,
301 spatially uniform hydraulic properties, and (in the TGB case), the absence of a streambed
302 conductance layer.

303 **2.4. Numerical perturbation-based CSD solution**

304 The perturbation method of estimating cumulative streamflow depletion resulting from
305 groundwater extraction at a given location and for a given duration involves the calculation of
306 two solutions; i.e., the solutions of equation (9) with $Q_B = 0$, and with $Q_B > 0$. The total volume
307 of stream–aquifer exchange is calculated for each of (1) the reference case featuring zero
308 extraction [i.e., $V_S(t_f; h)$] and (2) for the perturbed case featuring non-zero extraction [i.e.,
309 $V_S(t_f; h, \mathbf{x}_B)$]. Cumulative streamflow depletion can then be calculated as the difference between
310 these two results as:

$$V_{CSD}(t_f; \mathbf{x}_B) = V_S(t_f; h, \mathbf{x}_B) - V_S(t_f; h) \quad (20)$$

311 When the number of potential extraction locations is large, the corresponding number of
312 evaluations of equation (20) will also be large. This process can be computationally expensive,
313 depending upon forward model runtimes, which depend partly upon how easily model
314 convergence can be achieved.

315 **2.5. Derivation of a numerical adjoint CSD solution**

316 The expression for cumulative streamflow depletion presented in equation (7) involves
317 the integration of the sensitivity of stream-aquifer exchange flux (Q_s) to the rate of groundwater
318 extraction (Q_B) at a single given location of extraction (x_B). By integrating this over the duration
319 of extraction and then multiplying by Q_B, the resulting volume of CSD can be calculated. In

contrast, the key benefit of the adjoint state approach is the ability to evaluate the volume of cumulative streamflow depletion resulting from extraction from a single well at any potential location. In this context, the adjoint state variable $[\psi^*(\mathbf{x},t)]$ represents the sensitivity of stream-aquifer exchange flux to the rate of groundwater extraction at any location **x**. For this reason, it can replace the integrand in equation (7); i.e.:

$$V_{CSD}(t_f;\mathbf{x}) = Q_B \int_{t_f}^{t_0} \psi^*(\mathbf{x},t)\,dt = Q_B \int_{t_0}^{t_f} \psi^*(\mathbf{x},t_f - t)\,dt = Q_B \int_{0}^{\tau_f} \psi^*(\mathbf{x},\tau)\,d\tau \tag{21}$$

where is the adjoint state variable (ψ^*) is obtained from solution of the adjoint equation of equation (8) (described by equations 22−26 below). For convenience, an alternative independent variable, τ, is also introduced here and represents backwards time, defined as $\tau = t_f - t$. Full details of the derivation of equation (21) are provided in Electronic Supplementary Material S2. This expression states that, for any given extraction well location, the volume of cumulative streamflow depletion can be calculated as the temporal integral of the adjoint state variable at that well location. For this reason, CSD resulting from extraction at any potential location **x** can be predicted using a single adjoint state model run. The governing equation for the adjoint state model was defined as:

$$S_y \frac{\partial \psi^*(\mathbf{x},\tau)}{\partial \tau} + \nabla \cdot [\mathbf{T}\,\nabla\psi^*(\mathbf{x},\tau)] - \frac{K_S}{b_S} A_S(\mathbf{x})[\psi^*(\mathbf{x},\tau) - 1] = 0 \tag{22}$$

with boundary conditions:

$$\psi^*(\mathbf{x},\tau) = 0 \text{ where } \mathbf{x} = \Gamma_1 \tag{23}$$

$$\nabla\psi^*(\mathbf{x},\tau)\cdot\mathbf{n} = 0 \text{ where } \mathbf{x} = \Gamma_2 \tag{24}$$

$$[\alpha\,\psi^*(\mathbf{x},\tau) - \mathbf{T}\,\nabla\psi^*(\mathbf{x},\tau)]\cdot\mathbf{n} = 0 \text{ where } \mathbf{x} = \Gamma_3 \tag{25}$$

and the terminal condition:

$$\psi^*(\mathbf{x},\tau) = 0 \text{ where } \tau = t_f - t_f = 0 \quad (26)$$

The form of the governing equation for the adjoint state model (equation 22) is similar to that of the forward model (equation 9), with the following exceptions. The dependent variable used in the adjoint state model is backwards time (i.e., τ), rather than forward time (i.e., t). This substitution allows the specification of terminal conditions (where t=t_f and τ=0), rather than initial conditions (where t=t_0 and τ=$t_f - t_0$). Spatially distributed source/sink terms (i.e., N, including recharge) do not appear in the governing equation for the adjoint state model, as these are not dependent upon the rate of groundwater extraction (i.e., $\partial N/\partial Q_B = 0$). The groundwater extraction term itself was replaced by a value of unity (since $\partial Q_B/\partial Q_B = 1$) and was subsequently incorporated into the loading term, which was defined as:

$$\left(\frac{K_S}{b_S}\right) A_S(\mathbf{x})[\psi^*(\mathbf{x},\tau) - 1] \quad (27)$$

If equation (22) is divided through by specific yield (i.e., if the value of specific yield is spatially uniform), the loading term then becomes:

$$\left(\frac{K_S}{b_S\, S_y}\right) A_S(\mathbf{x})[\psi^*(\mathbf{x},\tau) - 1] \quad (288)$$

Prior to numerical solution, the adjoint state variable was rescaled linearly and an offset was applied as:

$$\Psi^*(\mathbf{x},\tau) = \psi^*(\mathbf{x},\tau)\,\gamma + \beta \quad (29)$$

The scaling parameter (γ) is the inverse of that used by Neupauer and Griebling (2012) and Griebling and Neupauer (2013). This alternative formulation was preferred as it better clarifies the linear transformation from ψ^* to Ψ^* during model pre-processing (and, conversely, from Ψ^* to ψ^* during the post-processing of model outputs). There are two reasons for this adjustment (Neupauer and Griebling, 2012; Griebling and Neupauer, 2013). First, for certain parameter

values, the magnitude of the loading term will be small with respect to numerical solution precision. Similarly, the spatial gradient of the adjoint state in the local vicinity of the loading term may also be small in relative terms. Therefore, a scaling parameter (γ) was used to increase the magnitude of the loading term. Second, depending upon the reference datum used in the vertical plane, the value of the loading term may be smaller than the specified bottom of the aquifer elevation. Therefore, an offset parameter (β) was used to ensure that loading term values were always larger than bottom of aquifer elevations.

In the next section, the accuracy of the new analytical and numerical adjoint solutions for CSD were demonstrated using a simple synthetic test case through comparisons to an equivalent numerical forward model, as well as to the numerical integration of ISD analytical solutions for instantaneous streamflow depletion. The efficacy of the new numerical adjoint solution for the prediction of CSD in more complex contexts is subsequently demonstrated through application to a numerical groundwater flow model of the Gloucester River Basin alluvial aquifer in New South Wales, Australia.

3. Synthetic demonstration

Neupauer and Griebling (2012) presented a conceptual model to demonstrate an adjoint solution for instantaneous streamflow depletion (Figure 2). In the present study, this model was modified to facilitate comparisons to numerical integration of analytical solutions. Specifically, the two-sided Neupauer and Griebling solution was simplified to a single-sided solution by using a Cauchy boundary condition (BC) to represent a stream on one side of the model domain. Dirichlet BCs were specified on all other boundaries. Model outputs were checked to ensure that inflows did not occur through Dirichlet boundaries. This arrangement of BCs was consistent with

an infinite aquifer extent, as assumed by the analytical streamflow depletion solutions to which numerical model results were compared.

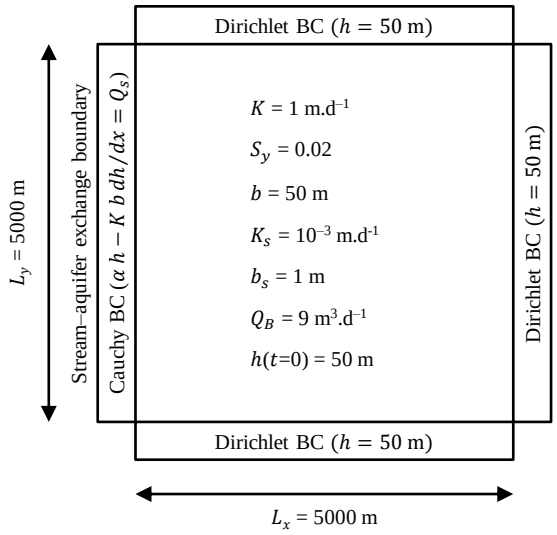

Figure 2. Synthetic groundwater flow model boundary conditions, initial condition, and parameterization, modified from the demonstration model previously presented by Neupauer and Griebling (2012).

Initial hydraulic head values were set equal to the aquifer top elevation to ensure equilibrium with Dirichlet boundary conditions. This specification also served, in combination with the use of conservative extraction rates, to ensure that desaturated conditions (i.e., hydraulic heads below base of aquifer elevations) were not induced. The stage parameter of the Cauchy BC representing the stream was also set equal to the aquifer top elevation to ensure equilibrium initial conditions, and therefore consistency with the analytical solutions to which results were compared. Streambed elevations were set equal to the base of the aquifer (i.e., 0 m), to ensure consistency with the assumption of full stream penetration extent used by the TGB and Hantush solutions. For the TGB conceptualization, streambed hydraulic conductivity was specified equal to aquifer hydraulic conductivity. Conversely, for the Hantush conceptualization, streambed hydraulic conductivity was specified as three orders of magnitude smaller than aquifer hydraulic

conductivity. Model outputs were generated at every time step. For adjoint state model simulations, scale and offset parameter values were set to γ=100 (–) and β=200 m respectively.

All numerical solutions (both forward and adjoint) were computed using the finite-difference flow simulator MODFLOW-2005 (Harbaugh, 2005). The model domain was discretized using spatially uniform cell dimensions of 50 m × 50 m × 50 m, resulting in a total of 100 rows and 100 columns. A simulated duration of 365 days was discretized using a uniform time step of 1 day, resulting in a total of 365 stress periods. The numerical solution was computed using the preconditioned conjugate gradient solver (Hill, 1990). Solver convergence criteria of 10^{-3} m and 10^{-3} $m^3.d^{-1}$ were specified for hydraulic head and flux calculations, respectively.

For the conceptualization featuring a fully penetrating stream without a conductance layer present, numerical integration of the TGB ISD analytical solution (equation 4) was used as the basis for comparisons (Figure 3a-c). For the conceptualization featuring a fully penetrating stream with a conductance layer present, numerical integration of the Hantush ISD analytical solution (equation 5) was used (Figure 3d-f). For the conceptualization featuring a partially penetrating stream with conductance layer present, numerical integration of the Hunt ISD analytical solution was used (equation 6) (Figure 3g-i). The analytical CSD solution was in near-exact agreement with the numerical integration of ISD solutions in all three conceptualizations (Figure 3a, 3d, 3g). In percentage terms, numerical CSD solutions were in near-exact agreement with numerical integration of ISD solutions when extraction occurred less than 3 km from the stream boundary condition (Figure 3b, 3e, 3h). However, these were associated with discrepancies of relatively small magnitude (Figure 3c, 3f, 3i). Therefore, in practical terms, these percent discrepancies were not substantial.

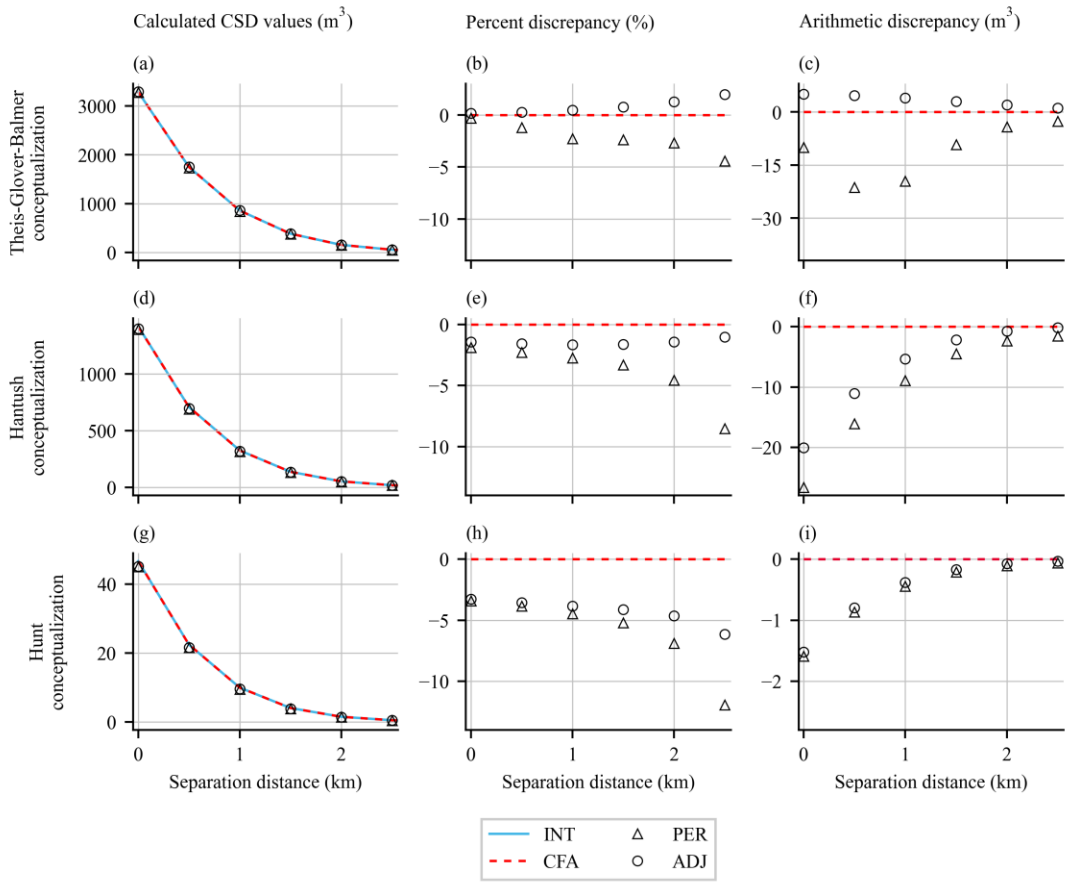

Figure 3. Analytical and numerical solutions for cumulative streamflow depletion (first column) and corresponding discrepancies with respect to numerical integration of ISD solutions, in percentage terms (second column) and as raw values (third column). All results are presented as functions of well-stream separation distance. (a-c) streambed conductance layer absent (Theis-Glover-Balmer conceptualization); (d-f) streambed conductance layer present (Hantush conceptualization); (g-i) streambed conductance layer present and stream partially penetrating the aquifer (Hunt conceptualization). Extraction well to stream distances were oriented perpendicular to the stream orientation. Abbreviations used: INT=numerical integration of analytical ISD solution; CFA=closed-form analytical CSD solution; PER=numerical perturbation-based solution; ADJ=numerical adjoint state solution.

4. Case study

To demonstrate the suitability of the numerical adjoint approach for the estimation of cumulative streamflow depletion, the method was applied to an existing numerical groundwater flow model of the Gloucester Basin, Australia (Peeters et al., 2018). The Gloucester sedimentary

basin is located approximately 200 km north-northeast of the city of Sydney in New South Wales, Australia. The region features a sub-tropical climate with a mean annual rainfall of 1100 mm and annual pan evaporation ranging from 1400 to 1700 mm. The Gloucester Basin contains up to 2500 m of faulted, deformed, and eroded coal-bearing Permian sedimentary and volcanic rocks located along a sinuous north to northeast-oriented strike. The basin is entirely bounded by outcropping Carboniferous basement rocks. In the north of the basin the Avon River enters from the west and flows northward through the towns of Stratford and Gloucester before discharging into the Gloucester River at a confluence that also includes the Barrington River. Mean annual streamflow of 177×10^6 m^3 occurs in the Avon River. An alluvial aquifer associated with the Avon River served as the case study for the present study. This aquifer is composed of Quaternary sediments ranging in size from clays to gravels, the total vertical thickness of which ranges up to 15 m. This aquifer is incised into the underlying basement geology and consequently its spatial extent is limited, with a maximum separation distance of approximately one kilometer between the stream network and the nearest aquifer (no-flow) boundary. Mean annual diffuse net recharge to the alluvial aquifer was estimated at 1 % of rainfall; i.e., 11 mm. Mean annual rates of evapotranspiration from shallow groundwater are estimated to range up to 50 % of rainfall; i.e., up to 550 mm. Watertable elevations are less than one metre below ground surface in locations proximal to the river. Under common flow conditions, the Avon River is characterised as a gaining system; i.e., local groundwater flows are consistently oriented toward the river and its tributaries. Limited extraction from the alluvial aquifer currently occurs for stock and domestic water supply (McVicar et al., 2014; Dawes et al., 2018; Peeters et al., 2018).

As part of the Bioregional Assessments Program for the Australian Federal Government, Peeters et al. (2018) developed a numerical groundwater flow model of the alluvial aquifer

associated with the Avon River and its tributaries. The finite-difference flow simulator MODFLOW-2005 (Harbaugh, 2005) was used to solve the relevant form of the groundwater flow equation. The spatial extent of the alluvial aquifer was discretized using a uniform grid of 225 rows and 140 columns (Figure 4a). A total of 4448 active cells were used for model calculations, with uniform dimensions of 90 m x 90 m. While the top and bottom elevations of model cells were variable, all cells featured a consistent thickness (and therefore maximum saturated thickness) of 15 m. A period of 120 years of extraction was simulated, which was discretized using 1440 month-long steps. Hydraulic properties were represented using uniform values, with horizontal hydraulic conductivity = 1 $m.d^{-1}$ and specific yield = 16 %. Time-varying net recharge was represented by applying a spatially distributed flux to each model cell, which ranged from 0.4 to 0.7 mm per month. Evapotranspiration was represented as a head-dependent process, with a maximum rate of 3.213×10^{-4} $m.d^{-1}$ when hydraulic head was equal to ground surface and declined linearly to zero when hydraulic head was equal to or less than an extinction depth of 2 m below ground surface. Groundwater discharge to the Avon River and its tributaries was represented using third-type (i.e., head-dependent) boundary conditions at a total of 598 cells (Figure 4a), using a spatially uniform streambed conductance value of 0.6 $m.d^{-1}$. Due to a lack of historical surface water monitoring, spatially variable but constant-in-time river stage values were specified, based upon the interpolation of the limited gauging station data available (Peeters et al., 2018). Similarly, due to a lack of direct observations (e.g., from field testing), hydraulic properties were parameterized using spatially uniform values, as was streambed conductance.

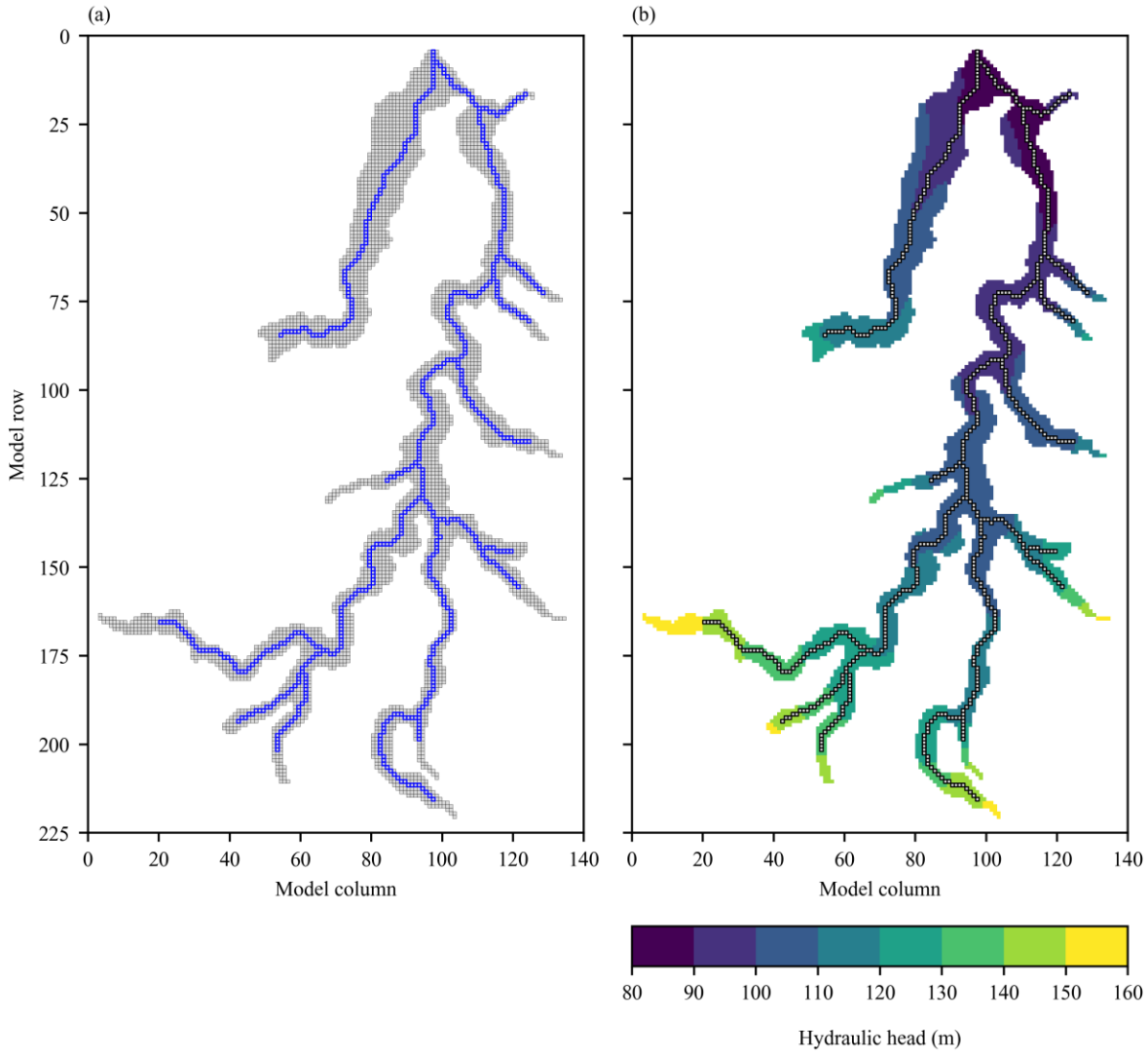

Figure 4. Numerical groundwater flow model of the Gloucester Basin alluvial aquifer. (a) Spatial discretization, with active cells represented by grey open squares and stream boundary conditions represented as blue open squares. (b) Spatial distribution of hydraulic head calculated by the forward model (from which extraction was excluded) after 120 years of simulation.

A number of modifications to the model described by Peeters et al. (2018) were undertaken to maximize the clarity of the adjoint state solution demonstration. In many cases, modifications also served to minimize model run times required for the calculation of perturbation-based results. These modifications to the forward model are described as follows.

The lower layer of the model (representing the basement rock aquifer) was removed, in order to avoid the need to specify a second adjoint state variable. The representation of head-dependent evapotranspiration by the EVT package was omitted, as it was inconsistent with the governing equation used to derive the adjoint state solution for CSD. Stream-aquifer exchange fluxes were represented by the RIV package rather than the DRN package. The latter did not permit the specification of river stage values, which was required to implement a constant source of adjoint state along the river network. The SIP solver was replaced by the PCG2 solver in order to maximize solution precision. Perhaps most importantly, the unconfined aquifer was simulated as being confined, in accordance with the Dupuit-Forchheimer assumption; i.e., that changes in saturated thickness (e.g., due to extraction) were small with respect to the total saturated thickness.

All numerical solutions (both forward and adjoint) were computed using the finite-difference flow simulator MODFLOW-2005 (Harbaugh, 2005), for which hydraulic head and flux convergence criteria of 10^{-3} m and 10^{-3} $m^3.d^{-1}$ were specified, respectively. The simulated groundwater flow field was generally oriented northwards, away from headwater areas at the southern extents of each alluvial valley (Figure 4b). The modelled spatial distribution of hydraulic heads was consistent with fully connected, gaining conditions at all locations along the Avon River and its tributaries. Model outputs were generated at every time step. Pre- and post-processing of model outputs was undertaken using the FloPy library for Python (Bakker et al., 2016). Additional model information, including discretization and parameterization details, are listed in Table 1.

502 **Table 1.** Gloucester Basin groundwater flow model summary, including discretization and parameterization details.

Parameter	Value	Units
Spatial extent (x,y)	20.25 × 12.60	km
Model cell size (x,y)	90 × 90	m
Spatial extent (z)	15	m
Model cell size (z)	15	m
Temporal extent	120	y
Time step length	30.4375	d
Number of active cells	4448	cells
Aquifer hydraulic conductivity, K	1	$m.d^{-1}$
Aquifer specific yield, S_y	16	%
Streambed conductance, C_s	0.6	$m.d^{-1}$
Extraction flux, Q_B	100	$m^3.d^{-1}$

503

504 The prediction of interest for this case study was the volume of cumulative streamflow
505 depletion resulting from groundwater extraction at a rate of 100 $m^3.d^{-1}$ (i.e., approximately equal
506 to 1.2 $L.s^{-1}$) at a single well located in any given cell in the model domain (other than the cells
507 representing the Avon River and its tributaries) over the simulated duration of 120 years. The
508 numerical adjoint solution was used to provide these predictions across the model domain. For
509 comparison purposes, predictions were also calculated using the perturbation approach, which
510 required a total of 3850 forward model runs. For adjoint state model simulations, scale and offset
511 parameter values were set to γ=100 (**–**) and β=200 m respectively.

512 Calculated cumulative streamflow depletion volumes were normalized by the total
513 extracted volume (i.e., 4.383×10^6 m^3) prior to analysis (Figure 5). Normalized CSD values
514 calculated from a total of 3850 model runs using the perturbation method ranged from near-zero
515 values at model cells distant from the stream network (purple cells) to a maximum of 0.972 at
516 model cells immediately adjacent to the river network (yellow cells) (Figure 5a). In comparison,

normalized CSD volumes calculated by a single adjoint state model run varied over an identical range and featured a consistent spatial distribution (Figure 5b).

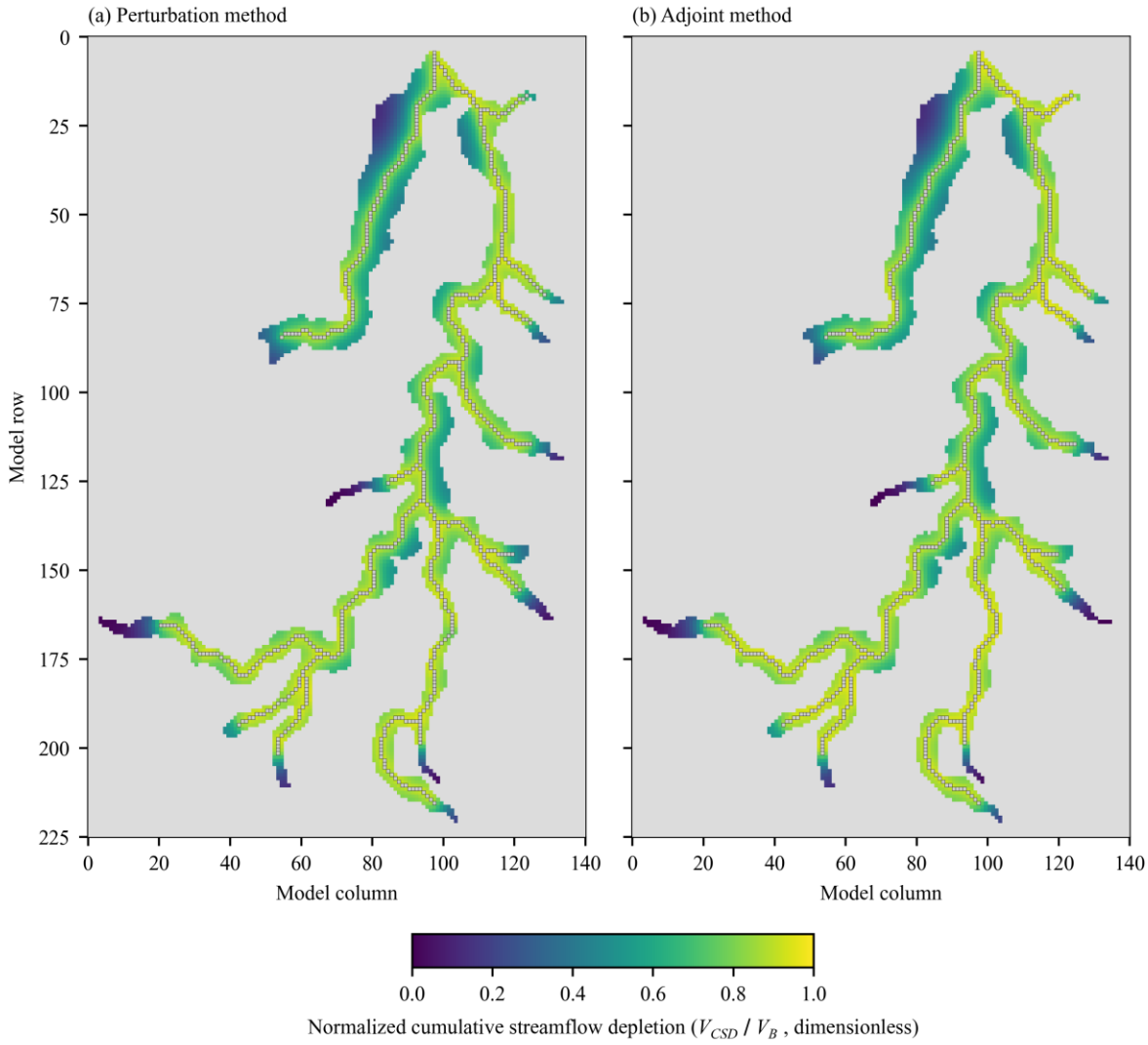

Figure 5. (a) Normalized cumulative streamflow depletion (V_{CSD}/V_B) resulting from single well extraction in the Gloucester Basin calculated via the perturbation method using 3850 numerical forward model runs. (b) Equivalent results calculated via an adjoint state solution using a single numerical adjoint model run. Model cells representing the Avon River network (which were not assessed as potential extraction locations) are represented as grey open squares.

Arithmetic differences between perturbation and adjoint method results ranged from -2×10^6 m^3 to $+14\times10^6$ m^3 (Figure 6a). All arithmetic difference values were relatively small (i.e., <1 %) with respect to the total volume of aquifer inflow (via recharge) over the simulated duration of 120 years; i.e., $\sim10^9$ m^3. Similarly, the majority (i.e., 93 %) of arithmetic difference values were relatively small (i.e., <5 %) with respect to the total volume of water extracted; i.e., 4.383×10^6 m^3. Percent difference values (defined as the discrepancy between adjoint and perturbation results, normalized by the latter results) ranged from –2 % to +55 % (Figure 6b). The majority (i.e., 92 %) of absolute percent difference values were less than 5 %. Three percent of percent difference values exceeded 10 %, the locations of which agreed with those where relatively large arithmetic differences were observed. More generally, the signs of arithmetic and percentage discrepancies were in agreement across the entirety of the active model domain.

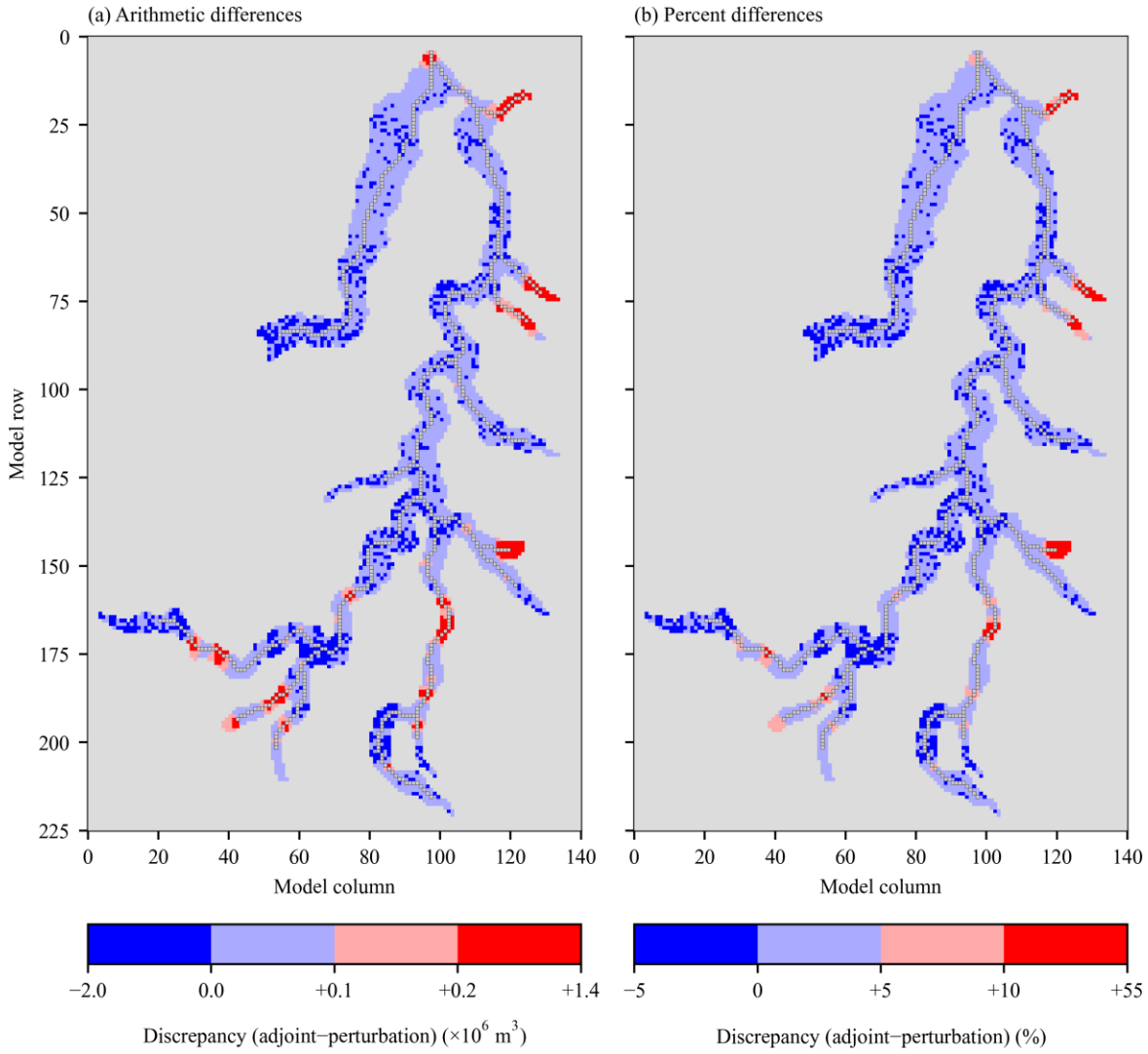

Figure 6. (a) Discrepancies between cumulative streamflow depletion volumes calculated via the perturbation and adjoint state methods, expressed as arithmetic differences. (b) Equivalent discrepancies expressed as percent differences, with respect to values calculated using the perturbation approach. Model cells representing the Avon River network (which were not assessed as potential extraction locations) are represented as grey open squares. Note: non-uniform color bar bin sizes were used to maximize figure information content.

5. Discussion

The results of the two case study applications are now discussed in terms of four themes, including the computational efficiency of the numerical adjoint method and insights derived

from the parameterization of the loading term in the adjoint state solution. Assumptions and limitations of the numerical adjoint solution are recognized, and potential broader applications of the numerical adjoint solution are also proposed.

5.1. Computational efficiency

In practical terms, the primary advantage of the adjoint state approach to CSD estimation was the substantial reduction in computational time achieved by avoiding the need to run a unique forward model in order to assess every potential extraction location. For the Gloucester Basin flow model, each single forward model run required approximately five seconds to achieve numerical convergence. In addition, approximately 25 seconds were required for the automated pre- and post-processing of each model via a Python language script. As the Gloucester Basin model contained 3850 active cells (excluding cells representing the Avon River and its tributaries), the evaluation of all potential extraction locations using the perturbation approach required approximately 27 hours in total to perform. The total time required when using the perturbation approach can be reduced through the use of parallel computing resources. In comparison, estimates of CSD resulting from all potential extraction locations were estimated simultaneously from a single numerical adjoint model run, which also required approximately five seconds to achieve numerical convergence.

5.2. Insights from the derivation of the numerical adjoint solution

In addition to computational advantages, an often-overlooked benefit of developing adjoint state solutions is the ability to derive closed-form expressions for the sensitivity of a specified model output to a specified model input. For closed-form analytical solutions, similar expressions can be derived through direct differentiation of the governing equation. For more complex models, which require the use of numerical methods to solve ordinary or partial

differential equations, adjoint state solutions provide a similar benefit. Adjoint state solutions for model sensitivities typically include two key components: (1) a loading term, and (2) a set of steps for processing modelled outputs. The former is defined by the state of interest (e.g., pressure or flux), including whether it is an instantaneous measure (i.e., at a given location and time) or a cumulative measure (e.g., integrated along a boundary, over an area, or through time). In comparison, the latter is defined by the parameter of interest; e.g., hydraulic properties, or an imposed source/sink flux, such as groundwater extraction.

A numerical adjoint solution for instantaneous streamflow depletion (ISD) was previously derived by Neupauer and Griebling (2012) in which the loading term contained in the governing equation (specifically, by equation 28) was composed of three parameters: streambed hydraulic conductivity (K_s), streambed thickness (b_s) and aquifer specific yield (S_y). The identification of the significance of these three parameters to the estimation of ISD was consistent with past studies. For example, Sophocleous et al. (1995) used numerical models to demonstrate that fluxes through a third-type boundary (representing groundwater discharge to streams, for example) are most sensitive to the streambed conductance parameter. The presence of aquifer specific yield in the loading term is also consistent with the known influence of this parameter on the timing of responses to hydraulic perturbations more generally; for example, as observed in pumping and slug test responses (e.g., McElwee and Yukler, 1978).

Post-processing of adjoint model outputs in the present study simply required the integration (performed as a summation) of the adjoint state variable at the potential location of extraction over the simulated duration (equation 21). Unlike typical adjoint state solutions to groundwater flow problems (e.g., Sykes et al., 1985; Wilson and Metcalfe, 1985), this did not require the combination of adjoint state model outputs with those of an associated forward

model. The temporal integration of the adjoint state variable can be interpreted as follows. Early derivations of adjoint solutions in nuclear reactor engineering research interpreted the meaning of the adjoint state variable as an "importance" function (e.g., Weinberg, 1952; Lewins, 1965). That is, the adjoint state variable describes the importance of a given system state at a given location and time to a given sensitivity of interest. In the present study, the sensitivity of interest was cumulative streamflow depletion; i.e., the change in total stream-aquifer exchange volume to groundwater extraction at a given location and undertaken over a specified duration. Therefore, for any potential extraction location of interest, the value of the adjoint state at any given point in time can be interpreted as the "importance" of an observation of hydraulic head (at a given location and time) to the estimation of CSD.

5.3. Assumptions and limitations of the numerical adjoint CSD solution

It is generally acknowledged that best modelling practice includes making explicit the assumptions associated with a given solution (Saltelli et al., 2013; Saltelli et al., 2020). Assumptions used in the derivation and calculation of the numerical adjoint CSD solution included the following. Stream stage was assumed to be insensitive to extraction. This assumption is common to many existing ISD solutions and is not unique to the numerical adjoint solution for CSD presented in this study. The simulation of changes in stream stage resulting from extraction over time would require the modelling of a separate mass balance for the stream network. For example, this could be simulated using the streamflow routing (SFR) package (Prudic, 1989) for the MODFLOW family of groundwater flow simulation codes. A separate adjoint state variable relating to stream stage would then need to be defined and simulated independently. For example, Neupauer and Griebling (2013) implemented an adjoint state approach to instantaneous streamflow depletion estimation using the SFR package in a

MODFLOW-2000 model (Harbaugh et al., 2000). This implementation featured three adjoint state variables that each varied in space and time, representing unconfined hydraulic head, confined hydraulic head, and stream stage. The form of the adjoint state governing equation was not consistent with that of the corresponding forward model, which necessitated modification of the numerical simulation code. The computation time required by a single adjoint state model was approximately one order of magnitude larger than for the corresponding forward model. However, this was still smaller than the total runtime required for solution of the thousands of forward model runs required for an equivalent analysis using the perturbation approach. In summary, the application of the adjoint state approach described in the present study is not limited to forward models in which surface water stages are represented using stationary values. Instead, the complexity of the forward model will determine that of the adjoint state solution. For both forward and adjoint solutions, a compromise is always required between (a) the level of complexity (and therefore accuracy) of process representations and (b) the levels of both data availability to underpin model solutions and resources required to develop them.

Groundwater extraction was assumed to be continuous over simulated time. Extension of the numerical adjoint CSD solution to include discontinuous extraction would require convolution of the present adjoint state solute with a time-varying extraction function (e.g., Neupauer et al. [2023b], equation 11). Similarly, the numerical adjoint CSD solution derived here is not suitable to assess continued CSD following the cessation of extraction (Neupauer et al., 2023b). However, it should be noted that this is a limitation of the forward, rather than adjoint state, model used in the present study. If a suitable forward model of post-extraction depletion could be identified, then it would provide the basis for deriving a suitable adjoint state solution for CSD following the cessation of extraction.

637 The numerical adjoint method derived and presented in the present study does rely,
638 however, on one key assumption: the linearity of surface water-groundwater exchange responses
639 to variations in groundwater extraction. The linearity of this driver–response relationship
640 underpins the adjoint state approach and is also consistent with analytical ISD solutions.
641 Specifically, the system response to a perturbation applied at the observation of interest (in the
642 present study, the total reduction in groundwater discharge to a stream network, summed over
643 time) is proportional to the system response resulting from an applied perturbation (in the present
644 study, groundwater extraction). The simulation of confined (rather than unconfined) aquifer
645 conditions was required to ensure linearity, as was the linear parameterization of the third-type
646 boundary conditions to represent groundwater discharge to the stream network.

647 **5.4. Potential broader applications of the numerical adjoint CSD solution**

648 The forward models used in the present study for benchmarking and demonstration
649 purposes featured spatially uniform and isotropic parameterizations of aquifer thickness,
650 hydraulic conductivity, specific yield, and streambed conductance values. However, it should be
651 noted that applications of numerical adjoint solutions are not limited to flow models featuring
652 homogeneous parameterizations. Unlike many other groundwater flow-related performance
653 functions assessed using the adjoint state approach (e.g., Sykes et al., 1985; Metcalfe and
654 Wilson, 1985), the expression used to calculate CSD (equation 21) is a function of only the
655 adjoint state variable. It does not depend explicitly on the solution of the forward model
656 governing equation, upon which the adjoint solution is based. The approach to deriving a
657 numerical adjoint solution for CSD presented here is generally applicable to models featuring
658 heterogeneous parameterizations. However, relaxing the assumption of homogeneity (e.g., for
659 parameters such as aquifer or streambed hydraulic conductivity, or aquifer specific yield) would

require re-derivation of the adjoint state, in order to redefine the value of the loading term applied along the stream network.

Although the example presented in the present study featured a perennial gaining stream and a steady, continuous extraction rate, the numerical adjoint approach to CSD estimation is not limited to this specific scenario. The numerical adjoint solution is also appropriate for application to streams featuring non-monotonic interactions (i.e., fluctuations between gaining and losing type. Since the performance measure of interest (i.e., the volume of CSD) is a relative measure of change, it may represent any of the following: reductions in groundwater discharge to streams; a change from gaining to losing stream conditions; or an increase in aquifer recharge from streams. The key assumption here is that stream–aquifer exchanges remain fully hydraulically connected, irrespective of the extraction rate and duration applied. Rates of groundwater extraction were assumed to be constant and uniform in time. The numerical adjoint solution presented here used the same temporal discretization scheme as the equivalent forward model. For this reason, the numerical adjoint solution presented is also appropriate for assessments of CSD resulting from discontinuous rates of groundwater extraction. This would require the groundwater extraction term in the performance measure (equation 21) to be incorporated within the temporal integral as:

$$V_{CSD}(t_f;\mathbf{x}) = \int_{t_0}^{t_f} Q_B(\mathbf{x},t)\,\psi^*(\mathbf{x},t_f-t)\,dt = \int_{0}^{\tau_f} Q_B(\mathbf{x},\tau_f-\tau+t_0)\,\psi^*(\mathbf{x},\tau)\,d\tau \qquad (30)$$

This operation can be seen as the convolution of the dimensionless adjoint state variable with a time-varying (e.g., discontinuous) volumetric extraction rate. To the authors' knowledge, the sensitivity of groundwater flow model states (i.e., hydraulic head or flow rate) to time-

varying (including discontinuous) extraction has not been estimated using the adjoint state method in studies published to date.

6. Conclusions

The traditional metric of streamflow depletion describes the instantaneous change in the volumetric rate of aquifer–stream exchange and is appropriate when applied at local scales. However, conjunctive management of surface and groundwater resources at regional scales typically involves estimation of volumetric water balances, which are often averaged over finite time periods. This requires a streamflow depletion metric that can be expressed as a total net annual volume, which can then be related to other water balance components. For this reason, an alternative metric of streamflow depletion was considered in the present study: cumulative stream depletion (CSD). This described the total volumetric reduction in flow from an aquifer to a stream resulting from continuous groundwater extraction over a finite period, at the end of the extraction period.

A novel analytical solution for the prediction of CSD was derived, based upon a forward solution that accounted for streambed conductance and partial stream penetration. The solution can alternatively be parameterized to represent full stream penetration. A simplified version of the analytical solution was also presented, which excluded the effects of both partial stream penetration and streambed conductance. These analytical solutions for CSD are appropriate for use in data poor investigations and represent upper limits for CSD predictions.

Separately, a novel numerical solution for prediction of CSD was presented, based on the derivation and calculation of an adjoint state solution. The accuracy and efficiency of the numerical adjoint solution was demonstrated through applications to simple and complex

groundwater flow models. Numerical adjoint solution results were compared to those obtained from both (a) forward numerical models and (b) the newly derived closed-form analytical solutions. In all cases, the accuracy of numerical adjoint solutions was demonstrated. The parameterization of the loading term used in the adjoint state solution identified three parameters of relevance to CSD prediction. These were streambed hydraulic conductivity and thickness, both of which contribute to the lumped parameterization of streambed conductance, as well as aquifer specific yield, which controls the rate at which hydraulic perturbations propagate through an aquifer. These findings were consistent with past sensitivity analyses of streamflow depletion solutions (e.g., Sophocleous et al., 1995) and interpretations of hydraulic testing.

The numerical adjoint method relied on the assumption that groundwater discharge responses to variations in groundwater extraction were linear. The simplified representation of unconfined conditions using confined flow was required to ensure linearity, as was the use of linear third-type boundary conditions to represent groundwater discharge to the stream network. For these reasons, the numerical adjoint approach to CSD is unsuitable for applications to circumstances in which linearized conditions are not met. These may include when extraction results in considerable variation in aquifer saturated thickness, or when stream-aquifer exchange fluxes are a nonlinear function of hydraulic gradient.

The computational advantage of the numerical adjoint solution was highlighted, where a single numerical model can be used to predict CSD impacts from all potential groundwater extraction locations in the vicinity of a gaining stream network. In comparison to the use of many forward models to calculate impacts by difference, the reduction in computational time required was proportional to the number of potential extraction well locations. For the case study presented, a substantial reduction in model run time of approximately 27 hours (i.e., a reduction

of almost 100 %) was achieved. More generally, when the number of potential locations is large then similar reductions in model run times can be achieved when the adjoint state approach to CSD estimation is employed.

7. Acknowledgments

Funding of this work was supported by the Australian Commonwealth Government's Geological and Bioregional Assessments Program. This research did not receive any specific grant funding from agencies in the commercial or not-for-profit sectors. The authors thank Bob Anderssen for his assistance in deriving an early version of the closed-form analytical solution for cumulative streamflow depletion.

8. Open Research

All scripts (as Python language scripts and as Jupyter Notebooks) and related datasets used to generate the results presented in this study can be obtained from the public GitHub code repository located at:

https://github.com/christurnadge/streamflow_depletion_adjoint_sensitivities (Turnadge, 2024).

9. Table of symbols

Symbol	Units	Description
A_S	–	Dimensionless function with a value of unity along streams and zero elsewhere
b	L	Aquifer saturated thickness
b_S	L	Streambed thickness
C_S	$L.T^{-1}$	Streambed conductance
G	$\sqrt{T}$	$\sqrt{(\Delta x)^2\, S_y/(4\, K\, b)}$
H	$\sqrt{T^{-1}}$	$\sqrt{\lambda^2/\left(4\, S_y\, K\, b\right)}$
h	L	Aquifer hydraulic head
h_S	L	Stream stage elevation
K	$L.T^{-1}$	Aquifer hydraulic conductivity
K_S	$L.T^{-1}$	Streambed hydraulic conductivity
L_x	L	Numerical model domain extent in x-plane
L_y	L	Numerical model domain extent in y-plane
N	$L.T^{-1}$	Spatially distributed source/sink terms
Q_B	$L^3.T^{-1}$	Volumetric rate of well extraction
Q_S	$L^3.T^{-1}$	Volumetric rate of aquifer–stream exchange
Q_{ISD}	$L^3.T^{-1}$	Volumetric rate of instantaneous streamflow depletion
R	L	$K\, b_S/K_S$
S_y	–	Aquifer specific yield
T	$L^2.T^{-1}$	Aquifer transmissivity
t_0	T	Initial time; i.e., at which groundwater extraction commences
t_f	T	Final time; i.e., at which groundwater extraction ceases
W_S	L	Streambed width
V_B	L^3	Total well extraction volume
V_{CSD}	L^3	Cumulative streamflow depletion volume
V^*_{CSD}	–	Dimensionless cumulative streamflow depletion, defined as $V^*_{CSD} = V_S/V_B$
V_S	L^3	Total volume of stream–aquifer exchange
$\mathbf{x}_B$	[L, L]	Extraction well location vector
z_{bot}	L	Elevation of base of unconfined aquifer
α	$L.T^{-1}$	Cauchy boundary condition parameter
β	–	Adjoint state variable offset parameter for numerical simulation
γ	–	Adjoint state variable rescaling parameter for numerical simulation
λ	$L.T^{-1}$	Streambed leakance
ψ^*	–	Adjoint state variable
Ψ^*	–	Scale and offset parameters used during numerical adjoint simulation
τ	T	Backward time, with respect to the final time of simulation, where $\tau = t_f - t$

10. References

Ahlfeld, D. P., Mulvey, J. M., Pinder, G. F., and Wood, E. F. (1988a). Contaminated groundwater remediation design using simulation, optimization, and sensitivity theory: 1. Model development. Water Resources Research, 24(3), 431-441.

Ahlfeld, D. P., Mulvey, J. M., and Pinder, G. F. (1988b). Contaminated groundwater remediation design using simulation, optimization, and sensitivity theory: 2. Analysis of a field site. Water Resources Research, 24(3), 443-452.

Bakker, M., Post, V. E. A., Langevin, C. D., Hughes, J. D., White, J. T., Starn, J. J., and Fienen, M. N. (2016). Scripting MODFLOW model development using Python and FloPy. Groundwater, 54(5), 733-739.

Barlow, P. M., and Leake, S. A. (2012). Streamflow depletion by wells: Understanding and managing the effects of groundwater pumping on streamflow. U.S. Geological Survey Circular no. 1376, Reston, Virginia, U.S.A., 84p.

Bear, J. (1979). Hydraulics of Groundwater. Dover Publications, Mineola, New York, U.S.A., 569p.

Brunner, P., Simmons, C. T., Cook, P. G., and Therrien, R. (2010). Modeling surface water-groundwater interaction with MODFLOW: Some considerations. Groundwater, 48(2), 174-180.

Brunner, P., Cook, P. G., and Simmons, C. T. (2011). Disconnected surface water and groundwater: from theory to practice. Groundwater, 49(4), 460-467.

Butler, J. J., Zlotnik, V. A. and Tsou, M. S. (2001). Drawdown and stream depletion produced by pumping in the vicinity of a partially penetrating stream. Groundwater, 39(5), 651-659.

763 Butler, J. J., Zhan, X., and Zlotnik, V. A. (2007). Pumping-induced drawdown and stream
764 depletion in a leaky aquifer system. Groundwater, 45(2), 178-186.
765 Cacuci, D. G. (1981a). Sensitivity theory for nonlinear systems. I. Nonlinear functional analysis
766 approach. Journal of Mathematical Physics, 22(12), 2794-2802.
767 Cacuci, D. G. (1981b). Sensitivity theory for nonlinear systems. II. Extensions to additional
768 classes of responses. Journal of Mathematical Physics, 22(12), 2803-2812.
769 Cacuci, D. G. (2003). Sensitivity and Uncertainty Analysis. Volume 1: Theory. CRC Press,
770 London, UK, 285p.
771 Cacuci, D. G., Ionescu-Bujor, M., and Navon, I. M. (2005). Sensitivity and Uncertainty
772 Analysis. Volume 2: Applications to Large-Scale Systems. CRC Press, London, UK, 367p.
773 Carter, R. D., Kemp Jr, L. F., Pierce, A. C., and Williams, D. L. (1974). Performance matching
774 with constraints. Society of Petroleum Engineers Journal, 14(02), 187-196.
775 Chan, Y. K. (1976). Improved image-well technique for aquifer analysis. Journal of Hydrology,
776 29(1–2), 149-164.
777 Chan, Y. K., Mullineux, N., Reed, J. R., and Wells, G. G. (1978). Analytic solutions for
778 drawdowns in wedge-shaped artesian aquifers. Journal of Hydrology, 36, 233-246.
779 Chavent, G., Dupuy, M., and Lemmonier, P. (1975). History matching by use of optimal theory.
780 Society of Petroleum Engineers Journal, 15(01), 74-86.
781 Chen, X., and Yin, Y. (2004). Semianalytical solutions for stream depletion in partially
782 penetrating streams. Groundwater, 42(1), 92-96.
783 Christensen, S. (2000). On the estimation of stream flow depletion parameters by drawdown
784 analysis. Groundwater, 38(5), 726-734.

785 Darama, Y. (2001). An analytical solution for stream depletion by cyclic pumping of wells near
786 streams with semipervious beds. Groundwater, 39(1), 79-86.
787 Dawes, W. R., Macfarlane, C., McVicar, T. R., Wilkes, P. G., Rachakonda, P. K., Henderson, B.
788 L., Ford, J. H., Hayes, K. R., Holland, K. L., O'Grady, A. P., Marvanek, S. P., and
789 Schmidt, R. K. (2018) Conceptual modelling for the Gloucester subregion: Product 2.3 for
790 the Gloucester subregion from the Northern Sydney Basin Bioregional Assessment.
791 Department of the Environment and Energy, Bureau of Meteorology, CSIRO and
792 Geoscience Australia, Australia, 124p.
793 Fox, G. A. (2004). Evaluation of a stream aquifer analysis test using analytical solutions and
794 field data. Journal of the American Water Resources Association, 40(3), 755-763.
795 Fox, G. A., DuChateau, P., and Dumford, D. S. (2002). Analytical model for aquifer response
796 incorporating distributed stream leakage. Groundwater, 40(4), 378-384.
797 Fox, G. A., Heeren, D. M., and Kizer, M. A. (2011). Evaluation of a stream-aquifer analysis test
798 for deriving reach-scale streambed conductance. Transactions of the ASABE, 54(2), 473-
799 479.
800 Gandini, A. (1967). A generalized perturbation method for bi-linear functionals of the real and
801 adjoint neutron fluxes. Journal of Nuclear Energy, 21(10), 755-765.
802 Glover, R. E., and Balmer, G. G. (1954). River depletion resulting from pumping a well near a
803 river. Eos, Transactions American Geophysical Union, 35(3), 468-470.
804 Gradshteyn, I. S., and Ryzhik, I. M. (2007). Table of Integrals, Series, and Products. 7th edition.
805 Edited by Alan Jeffrey and Daniel Zwillinger. Academic Press, London, U.K., 1171p.
806 Griebling, S. A., and Neupauer, R. M. (2013). Adjoint modeling of stream depletion in
807 groundwater-surface water systems. Water Resources Research, 49(8), 4971-4984.

808 Hantush, M. S. (1965). Wells near streams with semipervious beds. Journal of Geophysical
809 Research, 70(12), 2829-2838.
810 Harbaugh, A. W., E. R. Banta, M. C. Hill, and M. G. McDonald (2000). MODFLOW-2000, the
811 U.S. Geological Survey Modular Ground-Water Model—User Guide to Modularization
812 Concepts and the Ground-Water Flow Process. Open-File Report 00-92, U.S. Geological
813 Survey, Reston, Virginia, U.S.A., 121p.
814 Harbaugh, A. W. (2005). MODFLOW-2005, the US Geological Survey modular ground-water
815 model: The ground-water flow process. Techniques and Methods report no. 6-A16, US
816 Department of the Interior, U.S. Geological Survey, Reston, Virginia, U.S.A., 253p.
817 Herron N. F., Crosbie, R. S., Viney, N. R., Peeters, L. J. M., and Zhang, Y. Q. (2018). Water
818 balance assessment for the Gloucester subregion: Product 2.5 for the Gloucester subregion
819 from the Northern Sydney Basin Bioregional Assessment. Department of the Environment
820 and Energy, Bureau of Meteorology, CSIRO and Geoscience Australia, Australia, 40p.
821 Hill, M. C. (1990). Preconditioned conjugate-gradient 2 (PGC2), a computer program for solving
822 groundwater flow equations. Water Resources Investigations report 90-4048, U.S.
823 Geological Survey, Denver, Colorado, U.S.A., 43p.
824 Huang, C. S., and Yeh, H. D. (2015). Estimating stream filtration from a meandering stream
825 under the Robin condition. Water Resources Research, 51, 4848-4857.
826 Huang, C. S., Lin, W. S., and Yeh, H. D. (2014). Stream filtration induced by pumping in a
827 confined, unconfined or leaky aquifer bounded by two parallel streams or by a stream and
828 an impervious stratum. Journal of Hydrology, 513, 28-44.
829 Huang, C. S., Yang, T., and Yeh, H. D. (2018). Review of analytical models to stream depletion
830 induced by pumping: Guide to model selection. Journal of Hydrology, 561, 277-285.

831 Huang, C.S., Yang, S.Y., and Yeh, H.D. (2015). Technical Note: Approximate solution of
832 transient drawdown for constant-flux pumping at a partially penetrating well in a radial
833 two-zone confined aquifer. Hydrology and Earth System Sciences, 19, 2639-2647.
834 Hunt, B. (1999). Unsteady stream depletion from ground water pumping. Groundwater, 37(1),
835 98-102.
836 Hunt, B. (2003). Unsteady stream depletion when pumping from semiconfined aquifer. Journal
837 of Hydrologic Engineering, 8(1), 12-19.
838 Hunt, B. (2008). Stream depletion for streams and aquifers with finite widths. Journal of
839 Hydrologic Engineering, 13(2), 80-89.
840 Hunt, B. (2009). Stream depletion in a two-layer leaky aquifer system. Journal of Hydrologic
841 Engineering, 14(9), 895-903.
842 Hunt, B. (2014). Review of stream depletion solutions, behavior, and calculations. Journal of
843 Hydrologic Engineering, 19(1), 167-178.
844 Intaraprasong, T., and Zhan, H. B. (2009). A general framework of stream-aquifer interaction
845 caused by variable stream stages. Journal of Hydrology, 373(12), 112-121.
846 Jacquard, P. and Jain, C. (1965). Permeability distribution from field pressure data. Society of
847 Petroleum Engineers Journal, 5(04), 281-294.
848 Jenkins, C. T. (1968). Techniques for computing rate and volume of stream depletion by wells.
849 Groundwater, 6(2), 37-46.
850 Kabala, Z. J., and Milly, P. C. D. (1990). Sensitivity analysis of flow in unsaturated
851 heterogeneous porous media: Theory, numerical model, and its verification. Water
852 Resources Research, 26(4), 593-610.

Lehmann, F., and Ackerer, P. (1997). Determining soil hydraulic properties by inverse method in one-dimensional unsaturated flow. Journal of Environmental Quality, 26(1), 76-81.

Lewins, J. (1965). Importance, the adjoint function: The Physical Basis of the Variational and Perturbation Theory in Transport and Diffusion Problems. Pergamon Press, New York, U.S.A., 172p.

Lough, H. K., and Hunt, B. (2006). Pumping test evaluation of stream depletion parameters. Groundwater, 44(4), 540-546.

Marchuk, G. I. (1975). Formulation of the theory of perturbations for complicated models. Applied Mathematics and Optimization, 2(1), 1-33.

Marchuk, G. I. (1994). Adjoint equations and analysis of complex systems. Kluwer Academic Publishers, Boston, Massachusetts, U.S.A., 466p.

McElwee, C. D., and Yukler, M. A. (1978). Sensitivity of groundwater models with respect to variations in transmissivity and storage. Water Resources Research, 14(3), 451-459.

McVicar, T. R., Langhi, L., Barron, O. V., Rachakonda, P. K., Zhang, Y. Q., Dawes, W. R., MacFarlane, C., Holland, K. L., Wilkes, P. G., Raisbeck-Brown, N., Marvanek, S. P., Li, L. T., and Van Niel, T. G. (2014). Context statement for the Gloucester subregion: Product 1.1 from the Northern Sydney Basin Bioregional Assessment. Department of the Environment, Bureau of Meteorology, CSIRO and Geoscience Australia, Australia, 104p.

Mehl, S., and Hill, M. C. (2010). Grid-size dependence of Cauchy boundary conditions used to simulate stream–aquifer interactions. Advances in Water Resources, 33(4), 430-442.

Miller, C. D., Durnford, D., Halstead, M. R., Altenhofen, J., and Flory, V. (2007). Stream depletion in alluvial valleys using the SDF semianalytical model. Groundwater, 45(4), 506-514.

Neuman, S. P., and Yakowitz, S. (1980). A statistical approach to the inverse problem of aquifer hydrology: 1. Theory. Water Resources Research, 15(4), 845-860.

Neuman, S. P., Fogg, G. E., and Jacobson, E. A. (1980). A statistical approach to the inverse problem of aquifer hydrology: 2. Case study. Water Resources Research, 16(1), 33-58.

Neupauer, R. M., and Griebling, S. A. (2012). Adjoint simulation of stream depletion due to aquifer pumping. Groundwater, 50(5), 746-753.

Neupauer, R. M., and Wilson, J. L. (1999). Adjoint method for obtaining backward-in-time location and travel time probabilities of a conservative groundwater contaminant. Water Resources Research, 35(11), 3389-3398.

Neupauer, R. M., and Wilson, J. L. (2001). Adjoint-derived location and travel time probabilities for a multidimensional groundwater system. Water Resources Research, 37(6), 1657-1668.

Neupauer, R.M., Lackey, G. D., and Pitlick, J. (2021). Exaggerated stream depletion in streams with spatio-temporally varying streambed conductance. Journal of Hydrologic Engineering, 26(2), 04020066, doi:10.1061/(ASCE)HE.1943-5584.0002043.

Neupauer, R.M., Okkonen, J., and Tyson, E. (2023a). Prevention of thermal pollution of groundwater near open loop geothermal systems. World Environmental and Water Resources Congress, American Society of Civil Engineers, Henderson, Nevada, U.S.A.

Neupauer, R. M., Turnadge, C., and Okkonen, J. (2023b). Forward and adjoint modeling of sensitivities to periodic forcings in groundwater flow and transport. Mathematical Geosciences, 55(8), 1217-1241.

Ng, E. W., and Geller, M. (1969). A table of integrals of the error functions. Journal of Research of the National Bureau of Standards - B. Mathematical Sciences, 73B(1), 1-20.

898 Peeters, L. J. M., Dawes, W. R., Rachakonda, P. R., Pagendam, D. E., Singh, R. M., Pickett, T.
899 W., Frery, E., Marvanek, S. P., and McVicar, T. R. (2018). Groundwater numerical
900 modelling for the Gloucester subregion: Product 2.6.2 for the Gloucester subregion from
901 the Northern Sydney Basin Bioregional Assessment. Department of the Environment and
902 Energy, Bureau of Meteorology, CSIRO and Geoscience Australia, Australia, 160p.
903 Prudic, D. E. (1989). Documentation of a Computer Program to Simulate Stream-Aquifer
904 Relations Using a Modular, Finite-Difference, Ground-Water Flow Model. Open-File
905 Report 88-729, U.S. Geological Survey, Carson City, Nevada, U.S.A., 120p.
906 Reeves, H. W. (2008). STRMDEPL08-An extended version of STRMDEPL with additional
907 analytical solutions to calculate streamflow depletion by nearby pumping wells. Open-File
908 Report 2008-1166, U.S. Geological Survey, Reston, Virginia, U.S.A., 22p.
909 Rushton, K. (1999). Discussion of "Unsteady stream depletion from ground water pumping" by
910 B. Hunt. Groundwater, 37(6), 805.
911 Saltelli, A., Bammer, G., Bruno, I., Charters, E., Di Fiore, M., Didier, E., Espeland, W. N., Kay,
912 J. Lo Piano, S., and Mayo, D. (2020). Five ways to ensure that models serve society: A
913 manifesto. Nature, 582, 482–484.
914 Saltelli, A., Guimaraes Pereira, Â., Van der Sluijs, J. P., and Funtowicz, S. (2013). What do I
915 make of your latinorum? Sensitivity auditing of mathematical modelling. International
916 Journal of Foresight and Innovation Policy, 9(2-3-4), 213-234.
917 Sedghi, M. M., Samani, N., and Sleep, B. (2009). Three-dimensional semi-analytical solution to
918 groundwater flow in confined and unconfined wedge-shaped aquifers. Advances in Water
919 Resources, 32(6), 925-935.

Sophocleous, M., Koussis, A., Martin, J. L., and Perkins, S. P. (1995). Evaluation of simplified stream-aquifer depletion models for water rights administration. Groundwater, 33(4), 579-588.

Sun, D. M., and Zhan, H. B. (2007). Pumping induced depletion from two streams. Advances in Water Resources, 30(4), 1016-1026.

Sykes, J. F., Wilson, J. L., and Andrews, R. W. (1985). Sensitivity analysis for steady state groundwater flow using adjoint operators. Water Resources Research, 21(3), 359-371.

Theis, C. V. (1941). The effect of a well on the flow of a nearby stream. Eos, Transactions American Geophysical Union, 22(3), 734-738.

Townley, L. R., and Wilson, J. L. (1985). Computationally efficient algorithms for parameter estimation and uncertainty propagation in numerical models of groundwater flow. Water Resources Research, 21(12), 1851-1860.

Tsou, P. R., Feng, Z. Y., Yeh, H. D., and Huang, C. S. (2010). Stream depletion rate with horizontal or slanted wells in confined aquifers near a stream. Hydrology and Earth System Sciences, 14(8), 1477-1485.

Turnadge, C. (2024). christurnadge/streamflow_depletion_adjoint_sensitivities (v1.1). [Software]. Zenodo. https://doi.org/10.5281/zenodo.10906143.

Vemuri, V., and Karplus, W. J. (1969). Identification of nonlinear parameters of ground water basins by hybrid computation. Water Resources Research, 5(1), 172-185.

Virtanen, P., Gommers, R., Oliphant, T. E., Haberland, M., Reddy, T., Cournapeau, D., Burovski, E., Peterson, P., Weckesser, W., Bright, J., van der Walt, S. J., Brett, M., Wilson, J., Millman, K. J., Mayorov, N., Nelson, A. R. J., Jones, E., Kern, R., Larson, E., Carey, . J., Polat, I., Feng, Y., Moore, E. W., VanderPlas, J., Laxalde, D., Perktold, J., Cimrman, R.,

Henriksen, I., Quintero, E. A., Harris, C. R., Archibald, A. M., Ribeiro, A. H., Pedregosa, F., and Van Mulbregt, P. (2020). SciPy 1.0: Fundamental algorithms for scientific computing in Python. Nature Methods, 17(3), 261-272.

Wallace, R. B., Darama, Y., and Annable, M. D. (1990). Stream depletion by cyclic pumping of wells. Water Resources Research, 26(6), 1263-1270.

Ward, N. D., and Falle, S. (2012). Simulation of a multilayer leaky aquifer with stream depletion. Journal of Hydrologic Engineering, 18(6), 619-629.

Ward, N. D., and Lough, H. (2011). Stream depletion from pumping a semiconfined aquifer in a two-layer leaky aquifer system. Journal of Hydrologic Engineering, 16(11), 955-959.

Weinberg, A. M. (1952). Current status of nuclear reactor theory. American Journal of Physics, 20(7), 401-412.

Weinberg, A. M. and Wigner, E. P. (1958). The Physical Theory of Neutron Chain Reactors. University of Chicago Press, Chicago, Illinois, U.S.A., 801p.

Wigner, E. P. (1945). Effect of small perturbations on pile period. Manhattan Project Report CP-G-3048.

Wilson, J. L., and Metcalfe, D. E. (1985). Illustration and verification of adjoint sensitivity theory for steady state groundwater flow. Water Resources Research, 21(11), 1602-1610.

Yeh, H. D., and Chang, Y. C. (2006). New analytical solutions for groundwater flow in wedge-shaped aquifers with various topographic boundary conditions. Advances in Water Resources, 29(3), 471-480.

Zipper, S. C., Gleeson, T., Kerr, B., Howard, J. K., Rohde, M. M., Carah, J., and Zimmerman, J. (2019). Rapid and accurate estimates of streamflow depletion caused by groundwater

965 pumping using analytical depletion functions. Water Resources Research, 55(7), 5807-
966 5829.
967 Zlotnik, V. A. (2004). A concept of maximum stream depletion rate for leaky aquifers in alluvial
968 valleys. Water Resources Research, 40(6).
969 Zlotnik, V. A. (2014). Analytical methods for assessment of land-use change effects on stream
970 runoff. Journal of Hydrologic Engineering, 20(7), 06014009-1–06014009-5.
971 Zlotnik, V. A., and Tartakovsky, D. M. (2008). Stream depletion by groundwater pumping in
972 leaky aquifers. Journal of Hydrologic Engineering, 13(2), 43-50.

Figure 1.

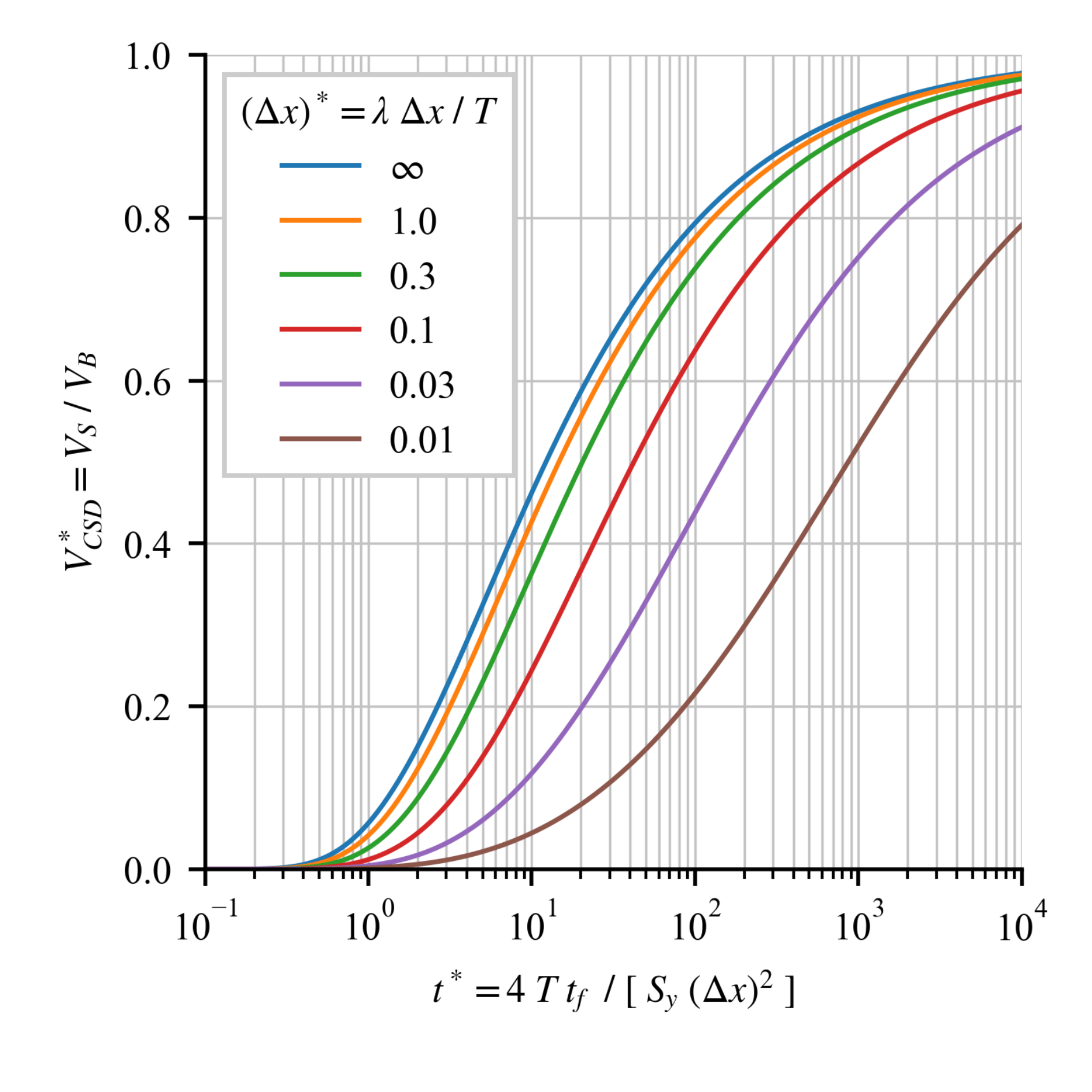
$(\Delta x)^* = \lambda\ \Delta x\ /\ T$
∞
1.0
0.3
0.1
0.03
0.01
$V^*_{CSD} = V_S\ /\ V_B$
1.0
0.8
0.6
0.4
0.2
0.0
10^{-1}
10^{0}
10^{1}
10^{2}
10^{3}
10^{4}
$t^* = 4\ T\ t_f\ /\ [\ S_y\ (\Delta x)^2\ ]$

Figure 2.

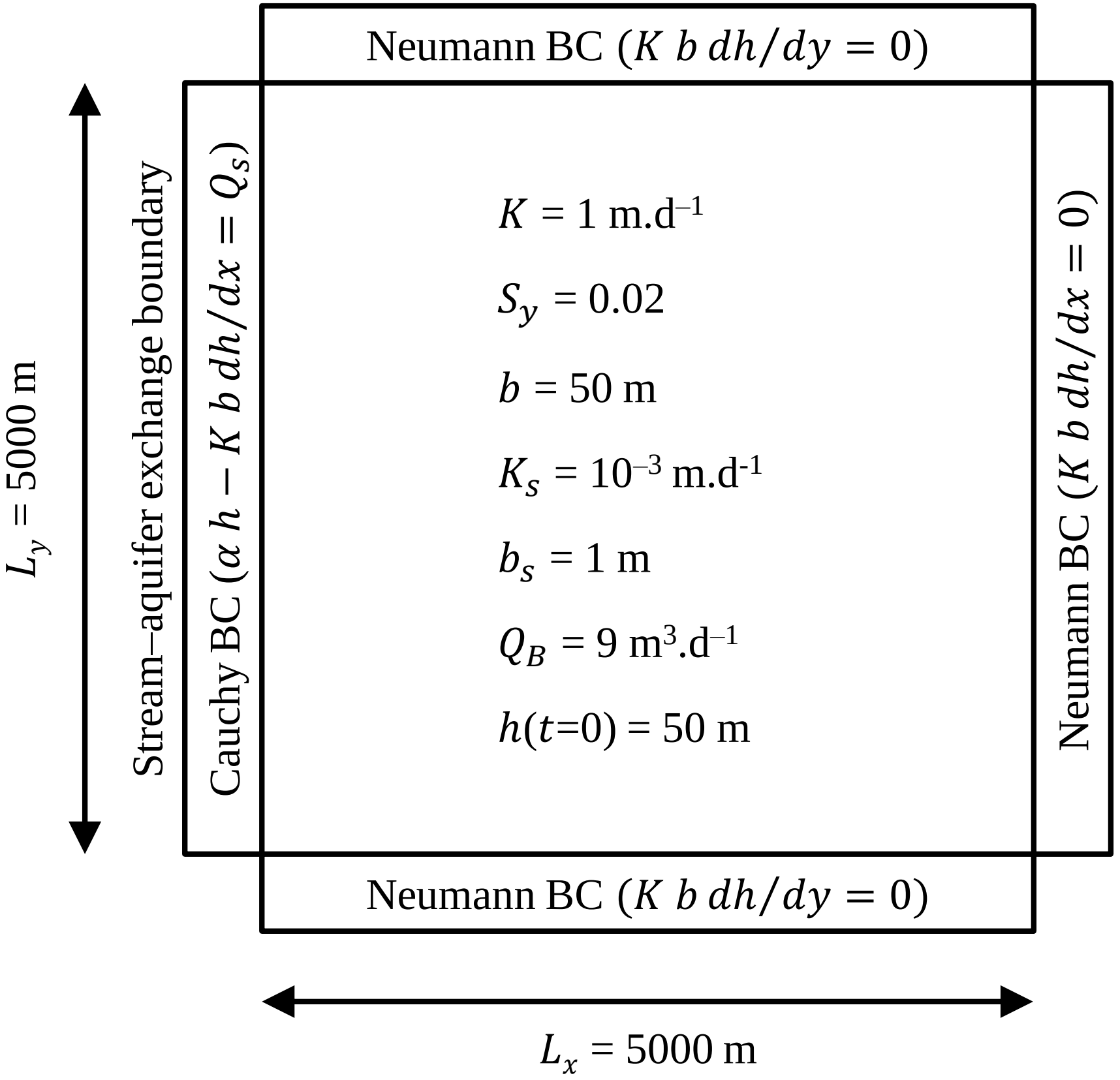
Neumann BC ($K\ b\ dh/dy = 0$)
Stream–aquifer exchange boundary
Cauchy BC ($\alpha\ h - K\ b\ dh/dx = Q_s$)
K = 1 m.d^{-1}
S_y = 0.02
b = 50 m
K_s = 10^{-3} m.d^{-1}
b_s = 1 m
Q_B = 9 m^3.d^{-1}
$h(t$=0) = 50 m
Neumann BC ($K\ b\ dh/dx = 0$)
Neumann BC ($K\ b\ dh/dy = 0$)
L_y = 5000 m
L_x = 5000 m

Figure 3.

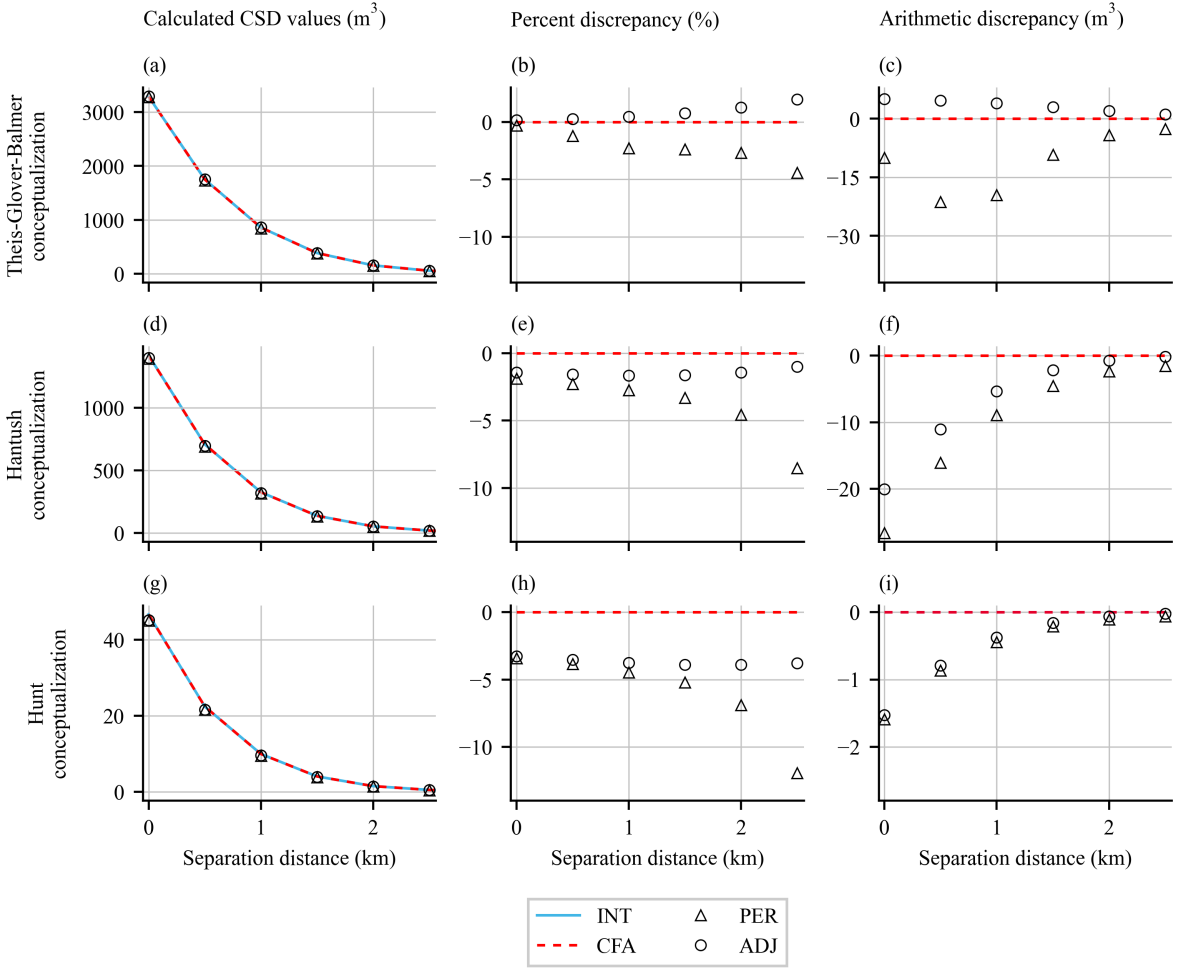
Calculated CSD values (m3)
Percent discrepancy (%)
Arithmetic discrepancy (m3)
Theis-Glover-Balmer conceptualization
Hantush conceptualization
Hunt conceptualization
(a)
(b)
(c)
(d)
(e)
(f)
(g)
(h)
(i)
3000
2000
1000
0
1000
500
40
20
−5
−10
−15
−20
−30
−1
−2
0
1
2
Separation distance (km)
INT
CFA
PER
ADJ

Figure 4.

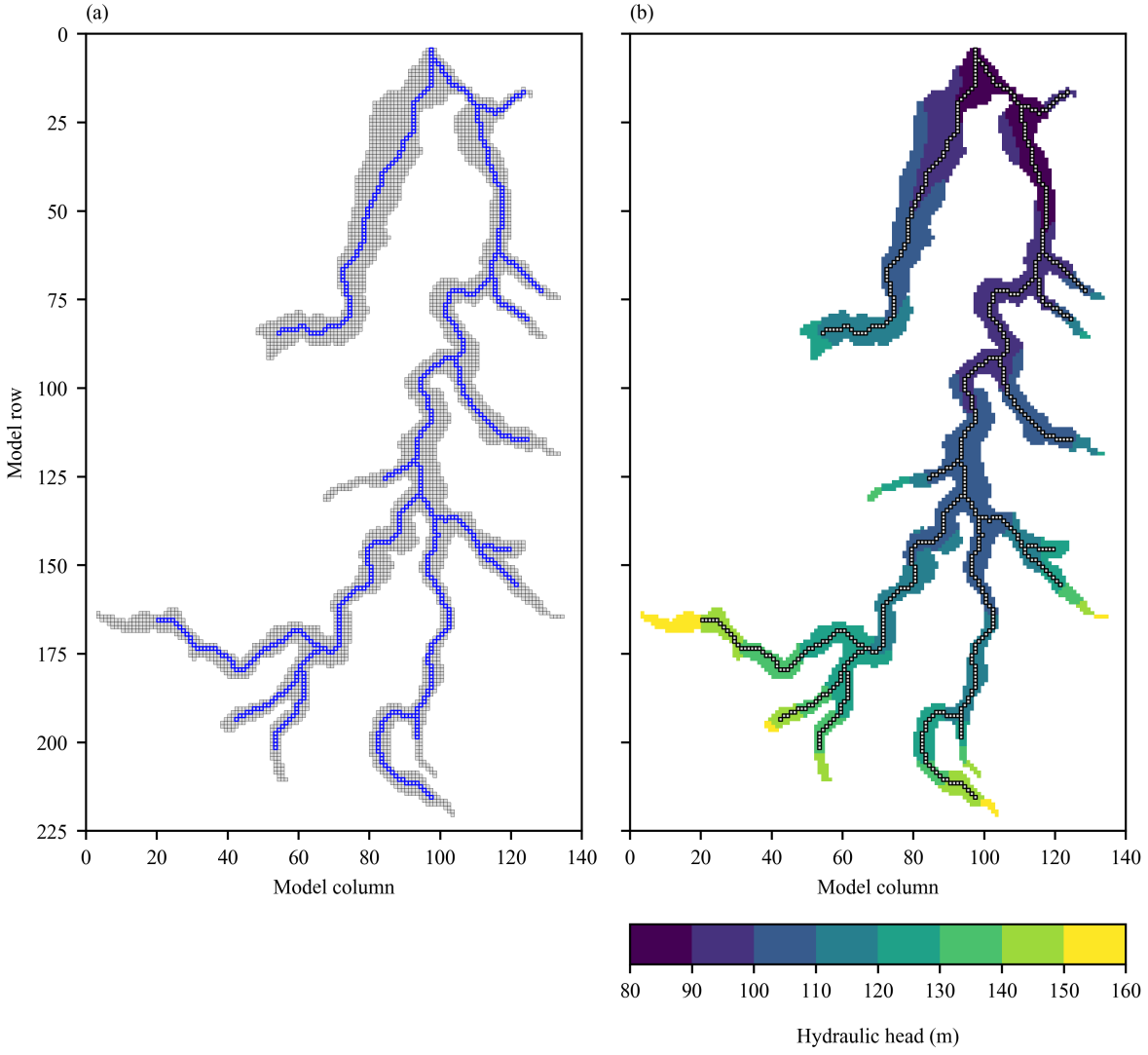
(a)
(b)
Model row
Model column
Model column
Hydraulic head (m)
0
25
50
75
100
125
150
175
200
225
0
20
40
60
80
100
120
140
80
90
100
110
120
130
140
150
160

Figure 5.

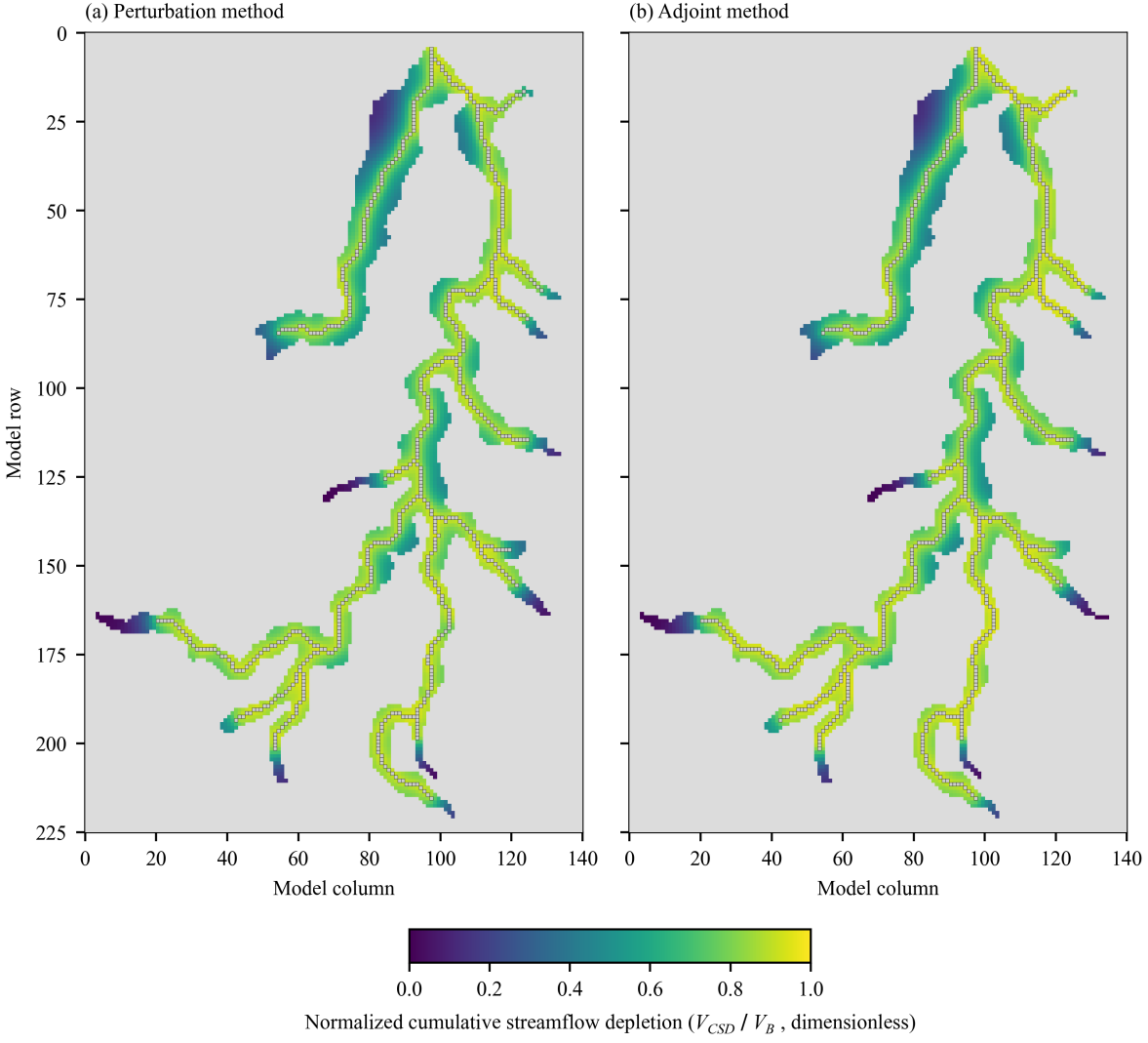
(a) Perturbation method
(b) Adjoint method
Model row
0
25
50
75
100
125
150
175
200
225
0
20
40
60
80
100
120
140
Model column
0.0
0.2
0.4
0.6
0.8
1.0
Normalized cumulative streamflow depletion (V_{CSD} / V_B , dimensionless)

Figure 6.

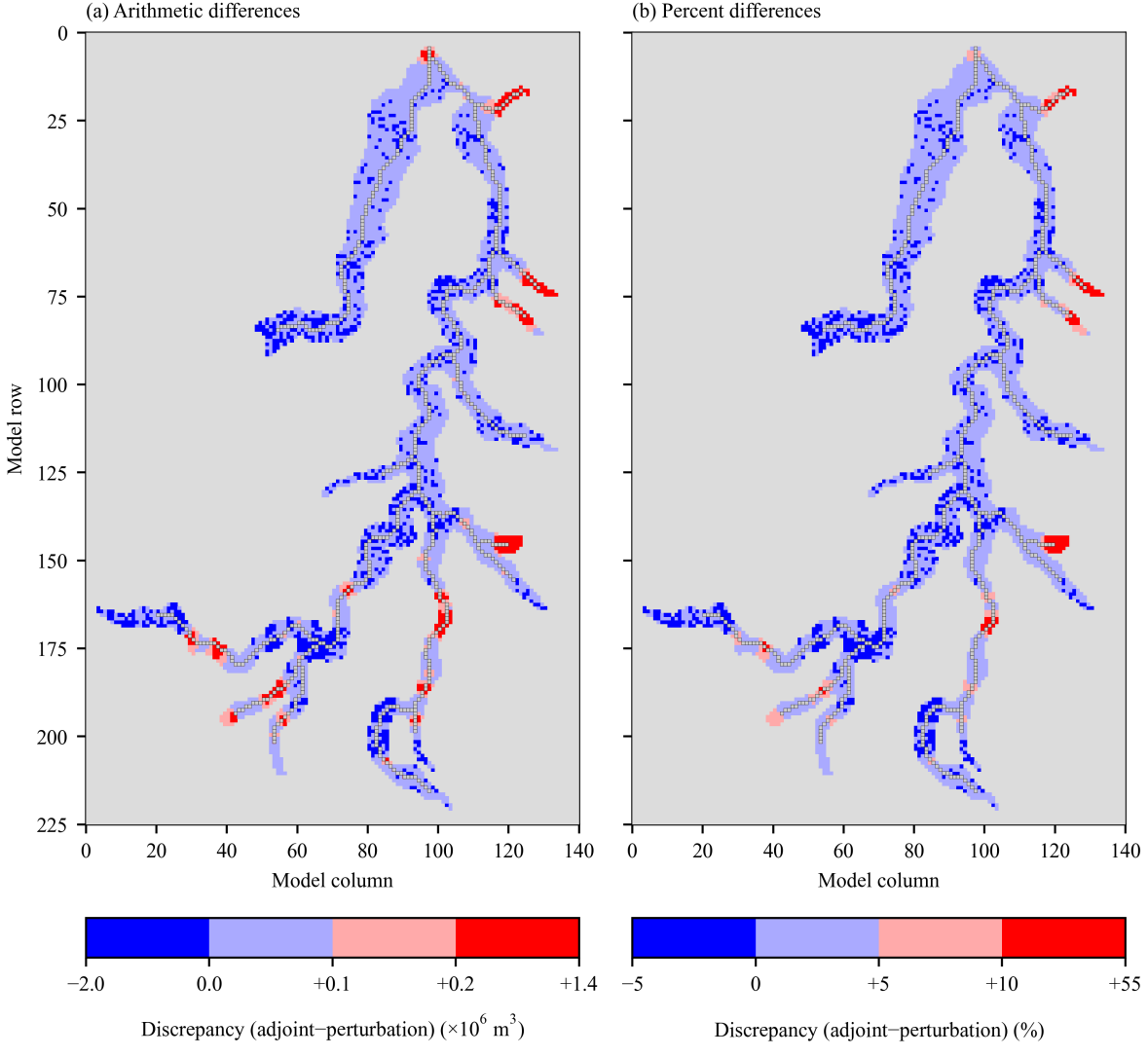
(a) Arithmetic differences
(b) Percent differences
Model row
0
25
50
75
100
125
150
175
200
225
0
20
40
60
80
100
120
140
Model column
−2.0
0.0
+0.1
+0.2
+1.4
Discrepancy (adjoint−perturbation) (×10^6 m^3)
−5
0
+5
+10
+55
Discrepancy (adjoint−perturbation) (%)